New Phytologist

Characterization of photosynthetic ferredoxin from the Antarctic alga *Chlamydomonas* sp. UWO241 reveals novel features of cold adaptation

Marina Cvetkovska[1], Beth Szyszka-Mroz[1], Marc Possmayer[1], Paula Pittock[2], Gilles Lajoie[2], David R. Smith[1] and Norman P. A. Hüner[1]

[1]Department of Biology and the Biotron Centre for Experimental Climate Change Research, University of Western Ontario, London, ON N6A 5B7, Canada; [2]Department of Biochemistry and Biological Mass Spectrometry Laboratory, University of Western Ontario, London, ON N6G 2V4, Canada

Author for correspondence:
Norman P. A. Hüner
Tel: +1 519 661 2111 ext. 86488
Email: nhuner@uwo.ca

Received: *12 September 2017*
Accepted: *27 March 2018*

New Phytologist (2018) **219:** 588–604
doi: 10.1111/nph.15194

Key words: *Chlamydomonas reinhardtii*, *Chlamydomonas* sp. UWO241, cold adaptation, ferredoxin, gene duplication, photosynthesis, protein activity and stability, psychrophily.

Summary

- The objective of this work was to characterize photosynthetic ferredoxin from the Antarctic green alga *Chlamydomonas* sp. UWO241, a key enzyme involved in distributing photosynthetic reducing power. We hypothesize that ferredoxin possesses characteristics typical of cold-adapted enzymes, namely increased structural flexibility and high activity at low temperatures, accompanied by low stability at moderate temperatures.
- To address this objective, we purified ferredoxin from UWO241 and characterized the temperature dependence of its enzymatic activity and protein conformation. The UWO241 ferredoxin protein, RNA, and DNA sequences were compared with homologous sequences from related organisms.
- We provide evidence for the duplication of the main ferredoxin gene in the UWO241 nuclear genome and the presence of two highly similar proteins. Ferredoxin from UWO241 has both high activity at low temperatures and high stability at moderate temperatures, representing a novel class of cold-adapted enzymes.
- Our study reveals novel insights into how photosynthesis functions in the cold. The presence of two distinct ferredoxin proteins in UWO241 could provide an adaptive advantage for survival at cold temperatures. The primary amino acid sequence of ferredoxin is highly conserved among photosynthetic species, and we suggest that subtle differences in sequence can lead to significant changes in activity at low temperatures.

Introduction

More than 70% of the Earth's biosphere is permanently at temperatures below 5°C. Primary production in many cold ecosystems is mainly dependent on photosynthetic microorganisms, including eukaryotic algae (Morgan-Kiss *et al.*, 2006). Many of these organisms are obligate cold-temperature extremophiles (psychrophiles), defined as being metabolically active and able to reproduce at temperatures permanently close to the freezing point of water and unable to tolerate more moderate (mesophilic) temperatures (≥ 20°C) (Cvetkovska *et al.*, 2017). Cold temperatures place severe physiochemical constraints on crucial aspects of cell function, including water viscosity, membrane fluidity, macromolecule interactions, and enzyme kinetics. Psychrophiles have evolved a complex collection of strategies to counteract the negative effects of low temperature. For example, psychrophiles require biological membranes with increased fluidity, antifreeze compounds that prevent intracellular ice crystal formation, and cold-adapted enzymes (Siddiqui *et al.*, 2013; De Maayer *et al.*, 2014).

Enzymes from psychrophiles are uniquely adapted to maintain high catalytic rates at low temperatures. The topic of psychrophilic protein structure and function has been extensively reviewed (D'Amico *et al.*, 2002; Feller & Gerday, 2003; Siddiqui & Cavicchioli, 2006; Siddiqui, 2017) and several broad adaptive trends have been described. For instance, the primary structure of enzymes from psychrophiles typically exhibits a set of general and specific changes (as compared with mesophilic homologues) that are hypothesized to confer higher structural flexibility, either globally or to the enzyme active site. A general theory for the types of structural adaptations that lead to increased cold activity is currently unavailable because different enzymes adopt their own strategies to improve protein flexibility (Feller, 2013; Åqvist *et al.*, 2017). Such adaptations can, however, lead to excessive flexibility at more moderate temperatures, causing the loss of activity at lower temperatures relative to their mesophilic counterparts (Feller & Gerday, 2003; Collins *et al.*, 2008).

Chlamydomonas sp. UWO241 (hereafter UWO241) is a unicellular green alga isolated 17 m below the surface of the permanently ice-covered Lake Bonney in Antarctica. This organism

persists in a highly stable environment characterized by permanently low temperatures (4–6°C), low irradiance (< 50 μmol photons m^{-2} s^{-1}) enriched in blue-green wavelengths (450–550 nm), and high salinities (700 mM) (Neale & Priscu, 1995). Under laboratory conditions, UWO241 grows optimally at 8°C and low salinity (70 mM), and is unable to grow at temperatures ≥18°C (Morgan *et al.*, 1998; Pocock *et al.*, 2004, 2007; Takizawa *et al.*, 2009; Possmayer *et al.*, 2011). With over two decades of research focused on the biochemistry and biophysics of its photosynthetic apparatus (Morgan-Kiss *et al.*, 2006; Dolhi *et al.*, 2013; Cvetkovska *et al.*, 2017), and a close phylogenetic relationship with other model algae such as *Chlamydomonas reinhardtii* and *Dunaliella salina* (Possmayer *et al.*, 2016), UWO241 is emerging as an attractive system for studying how photosynthesis operates at low temperatures. While some aspects of photosynthesis in UWO241 have been studied in detail, researchers have not yet managed to link these features to the function of cold-adapted enzymes.

Ferredoxins (Fds) are small, soluble iron-sulfur proteins ubiquitously present across all domains of life (Müller *et al.*, 1999; Fukuyama, 2004; Atkinson *et al.*, 2016). Photosynthetic Fds mediate electron transfer from the chloroplast electron transport chain (cETC) via photosystem I (PSI) to various essential metabolic reactions. These proteins are present as multiple isoforms in land plants and green algae, and are often expressed under different conditions (Terauchi *et al.*, 2009). Although plants and green algae have multiple Fds, members of the Fd gene family usually exhibit significant differences in their primary amino acid sequence. For example, *C. reinhardtii* encodes 13 Fd genes, which show 30–67% similarity with one another, and only six of which (FDX1-6) have been characterized in some detail (Terauchi *et al.*, 2009; Winkler *et al.*, 2010; Peden *et al.*, 2013; Yang *et al.*, 2015; Boehm *et al.*, 2016). Recently, a global interaction network was established for *C. reinhardtii*, providing putative roles for Fds in redox metabolism, carbohydrate modification, fatty acid biosynthesis, hydrogen production, nitrogen and sulfur metabolism, state transitions, and dark anoxia (Peden *et al.*, 2013). The best-characterized enzyme in this family is the photosynthetic Fd (PETF or Fd-1), the most abundant isoform, representing almost 98% of all Fd transripts in *C. reinhardtii* (Terauchi *et al.*, 2009). The main function of this protein is to transfer electrons from PSI to NADPH, via Fd : $NADP^+$ oxidoreductase (FNR), during linear electron flow (LEF), which contributes reducing power to carbon metabolism. In addition, PETF has been shown to interact with other protein partners, including chloroplast thioredoxins, sulfite reductase, nitrite reductase, hydrogenase, and glutamate synthase (Winkler *et al.*, 2010; Peden *et al.*, 2013). PETF also functions in cyclic electron flow (CEF), where electrons are passed from PSI to the cETC, via Fd and FNR, to prevent photoinhibition and photodamage under stressful conditions (Shikanai, 2007; Iwai *et al.*, 2010). Thus, Fd is a key enzyme involved in many aspects of photosynthesis and metabolism in green algae.

Here, we characterize photosynthetic Fd from UWO241. As proper functioning of Fd is dependent on its efficient interaction with many other proteins, we hypothesize that this enzyme is of key importance, and, accordingly, should exhibit characteristics typical of cold-adapted enzymes. Ultimately, we highlight potential adaptations of the UWO241 Fd to its unique and extreme Antarctic environment and argue that cold-adapted Fd provides an advantage for life at low temperatures.

Materials and Methods

Growth conditions

Chlamydomonas reinhardtii strain cc-1690 was grown axenically in Bold's Basal Medium (BBM) with 70 mM NaCl at 28°C, whereas *Chlamydomonas* sp. UWO241 was grown in BBM at 5°C, supplemented with 70 or 700 mM NaCl. All cultures were aerated continuously with ambient air filtered by sterile cotton batting in 4 l glass bottles. Growth irradiance of 150 mol photons m^{-2} s^{-1} was generated by fluorescent tubes (Sylvania CW-40; Osram-Sylvania, Mississauga, Canada) and measured with a quantum sensor attached to a radiometer (Model LI-189; Li-Cor, Lincoln, NE, USA). Mid-log cultures were used in all experiments.

Ferredoxin purification

Ferredoxin purification was performed as described by Terauchi *et al.* (2009) with minor modifications. Cells were centrifuged (3000 ***g***, 5 min) and resuspended in 100 ml of 20 mM Tricine-NaOH, pH 7.4, containing 50 mM NaCl. Cells were disrupted by a chilled French press at 6000 psi, and centrifuged (25 000 ***g***, 80 min, 4°C). The supernatant was treated with 1 μg ml^{-1} DNase I and 0.3% (w/v) streptomycin sulfate for 1 h at 5°C, centrifuged (25 000 ***g***, 30 min, 4°C), and dialyzed three times (1, 3, and 16 h) against 2 l of 20 mM Tricine-NaOH, with 2 mM β-mercaptoethanol (buffer A) containing 0.1 M NaCl. The solution was centrifuged (25 000 ***g***, 60 min, 4°C) and loaded onto a DE52 anion exchange column (15 × 2.5 cm) equilibrated with buffer A containing 0.1 M NaCl, and a NaCl gradient (0.1–1 M in buffer A, 120 ml) was applied. Reddish-colored fractions were collected, and protein samples were concentrated by centrifugation (Millipore Ultracel YM-3) to 5 ml. Thirty-five milliliters of buffer A were added to reduce salt concentration. Samples were loaded onto a Q-Sepharose anion exchange column (GE Healthcare, Pittsburg, PA, USA) (25 × 2.5 cm), equilibrated with buffer A containing 0.1 M NaCl, and a gradient of NaCl (0.1–1 M in buffer A, 120 ml) was applied. Reddish-colored fractions with $A_{422}/A_{280} > 0.3$ were collected and concentrated as described earlier. Samples were loaded onto a Sephacryl S-100 HR gel filtration column (GE Healthcare) (0.9 × 60 cm) equilibrated with buffer A, containing 0.1 M NaCl. Chromatographic runs were performed at a constant flow rate of 1 ml min^{-1}.

Sodium dodecyl sulfate-polyacrylamide gel electrophoresis (SDS-PAGE), immunoblotting and isoelectric focusing

Protein samples were solubilized with 2% (w/v) SDS and 1% (v/v) β-mercaptoethanol and loaded on either an equal protein basis (soluble fraction and purified Fd) or an equal Chl basis

(total fraction). Electrophoresis and protein transfer were performed as previously described (Szyszka-Mroz *et al.*, 2015). Membranes were probed with primary antibody specific for Fd from *C. reinhardtii* (1 : 1000; Agrisera, Vännäs, Sweden), and a horseradish peroxidase secondary antibody (Sigma; 1 : 10 000). The antibody-protein complexes were visualized using enhanced chemiluminescence detection reagents (GE Healthcare) as per the manufacturer's instructions. Protein amounts were quantified by densitometry using ImageJ (National Institutes of Health, Bethesda, MD, USA).

For isoelectric focusing (IEF), concentrated fractions of purified Fd were precipitated with four volumes of 100% acetone (1 h, −20°C). Samples were centrifuged, and the pellet was resuspended in 80% (v/v) acetone. After an additional centrifugation, the pellets were air-dried. IEF was performed as previously described (Szyszka-Mroz *et al.*, 2015) using the following settings: 30 min at 200 V, 15 min at 500 V, 15 min at 750 V, and 60 min at 1000 V.

Nano-LC-ESI-MS/MS

Isolated Fd proteins from *C. reinhardtii* and UWO241 were prepared for nano liquid chromatography tandem mass spectrometry (nano-LC-ESI-MS/MS) analysis as previously described (Szyszka-Mroz *et al.*, 2015) and digested with AspN and chymotrypsin. Fifty percent of each original sample was injected onto a MClassNanoAcquity ultra-performance liquid chromatograph (Waters) equipped with a 25 cm × 75 μm C18 reverse-phase column employing an 80 min LC gradient (5–37.5% (v/v) acetonitrile and 0.1% (v/v) formic acid) and detected in a data-dependent acquisition mode (Top 10, FT/FT/HCD) by tandem MS (QExactive; Thermo Scientific, Waltham, MA, USA), using the following acquisition parameters: survey scans range of 350–1800 mass-to-charge ratio, 70 000 MS resolution, and top 10 precursors selected based on charge state (+2, +3, and +4 ions). Tandem MS fragmentation was performed using higher-energy C-trap dissociation (HCD) fragmentation and acquired at 17 500 resolution. Raw data files were processed by PEAKS (Bioinformatics Solutions Inc., Waterloo, ON, Canada) for *de novo* sequencing and homology searching against the National Center for Biotechnology Information (NCBInr). The following settings were used: parent mass error tolerance of 20.0 ppm, fragment mass error tolerance of 0.05 Da, % false discovery rate (FDR) of 0.1% and three unique peptides, fixed modification for carbamidomethyl Cys, variable modification for oxyM, and deamidation N/Q.

Circular dichroism spectroscopy

Circular dichroism (CD) spectra were obtained using a Jasco J-810 spectropolarimeter (Jasco, Oklahoma City, OK, USA) equipped with a temperature control unit. The recorded far-UV spectra were the average of five scans obtained at a rate of 20 nm min^{-1}, response time of 2 s, and a bandwidth of 1 nm. Temperature-dependent melting curves were collected by measuring the protein ellipticity of purified Fd solutions (1 mg ml^{-1}), using a 1-mm-pathlength quartz cuvette. In these experiments, the temperature ranged from 5 to 80°C and increased at a rate of 1°C min^{-1}. CD spectra (200–260 nm) were taken every 5°C after 2 min equilibration time. Chemical denaturation experiments were carried out by measuring the ellipticity (210–260 nm) of purified Fd solutions (1 mg ml^{-1}) containing different concentrations of guanidine-HCl, using a 1-mm-pathlength quartz cuvette. In these experiments, the temperature was kept constant at 25°C for Fd from *C. reinhardtii* and 10°C for Fd from UWO241. In all cases, averaged spectra, corrected for the blank (25 mM Na-phosphate buffer, pH 7.8), were smoothed using the Savitzky–Golay algorithm. Final far-UV CD data were reported as mean residue ellipticity (MRE) (degrees cm^2 $dmol^{-1}$ per residue) or expressed as a change in MRE (relative units).

Ferredoxin-dependent cytochrome c reductase activity

Electron transfer between Fd and Fd-$NADP^+$ oxidoreductase (FNR) was measured indirectly as the reduction of cytochrome c by Fd (Terauchi *et al.*, 2009). Reactions (0.5 ml) containing 30 mM Tris-HCl (pH 7.8), 200 μM NADPH and 40 μM cytochrome c (bovine heart; Sigma) were incubated at room temperature for 30 min, followed by addition of 6 nM FNR (*Spinacia oleracea*, Sigma), and 3 μM of purified algal Fd. The reduction of cytochrome c was monitored immediately by measuring the increase in absorbance at 550 nm for 3 min at room temperature. Reaction rates were calculated using a molar absorption coefficient of 28 mM^{-1} cm^{-1}. To ensure that differences in the rate of reaction were not a result of using FNR and Fd from different species, the enzyme kinetics (K_m and V_{max}) were determined for Fd from *C. reinhardtii*, UWO241, and *S. oleracea*, ranging in concentration from 0.5 to 200 μM. The results were comparable between the algal species (Supporting Information Fig. S1).

Genome and transcriptome assembly

UWO241 cells were harvested by centrifugation (6000 ***g***, 5 min, 4°C), flash-frozen in liquid nitrogen, and stored at −80°C. Genomic DNA was extracted using Qiagen Plant DNeasy Maxi Kit (Qiagen) according to the manufacturer's instructions. The DNA was purified by ethanol precipitation using standard methods and resuspended in 10 mM Tris, pH 7.5. The quality of DNA was monitored using wavelength absorbance scan and electrophoresis on a 1% (w/v) TBE agarose gel. Genomic DNA was sequenced at the Princess Margaret Genomics Centre (Toronto, ON, Canada). DNA was fragmented using a Covaris M220 Focused-Ultrasonicator (Covaris, Woburn, MA, USA) and libraries were constructed with the TruSeq DNA HT Sample Preparation Kit (FC-121-2003; Illumina, San Diego, CA, USA). Sequencing was performed using 101-cycle paired-end reads at a 100× coverage using an Illumina HiSeq2000. The resulting data were processed to remove adapter sequences and to trim low-quality ends using cutadapt (Martin, 2011). Quake v.0.3 (Kelley *et al.*, 2010) was used to correct sequencing errors. The genome was assembled *de novo* using ABySS (v.1.5.2) (Simpson *et al.*, 2009).

RNA was isolated using a modified CTAB protocol (Possmayer *et al.*, 2016) and sequenced at the Genome Québec

Innovation Centre (Montreal, QC, Canada). Libraries were constructed with the TruSeq Stranded mRNA Library Prep Kit (Set A, RS-122-2101; Illumina), and sequencing was performed using 125 bp paired-end reads on the Illumina HiSeq2500 V4 platform. Datasets were processed to remove adapter sequences and portions of reads with low-quality scores using TRIMMOMATIC (Bolger *et al.*, 2014) and assembled with TRINITY (v.2.1.1) (Grabherr *et al.*, 2011).

Ferredoxin sequences from UWO241

The transcriptomic and genomic datasets were screened for the presence of Fd genes using BLAST searches with known Fd sequences from *C. reinhardtii*, and other algae and plants, and with the most conserved protein regions as determined by multiple sequence alignment analysis. UWO241 sequences with a high degree of identity (E-value cutoff 10^{-30}) were obtained and annotated using GENEIOUS v.9.1 (Biomatters Ltd, Auckland, New Zealand). The transcript and genomic sequences of Fd-1 from UWO241 were confirmed by Sanger sequencing using gene-specific primers (forward 5′-ATGCAGGTCAGCCGTG TTTCG-3′ and reverse 5′-TACGCGGGTGGCTTAGTAGA GGG-3′) with template RNA and DNA extracted as described earlier. Fd-1 sequences were amplified by PCR and resolved on 1% (w/v) agarose gels. Bands were excised and purified with a gel extraction kit (Qiagen). The resulting fragments were inserted into the pDONR221 vector (ThermoFisher Scientific, Waltham, MA, USA), following the manufacturer's instructions and cloned into DH5α *Escherichia coli* cells using standard protocols. Plasmids were extracted using a plasmid miniprep kit (Qiagen) and sequenced (Robarts Research Institute, London, ON, Canada).

Evolutionary analysis

To detect potential evolutionary selection of the Fd-1 proteins in UWO241, the $d_N : d_S$ (ω) value was calculated using the codeML program in phylogenetic analysis by maximum likelihood (PAML; Yang, 2007), using a translational alignment and a pairwise comparison between *C. reinhardtii* and UWO241 protein-coding sequences (one-ratio model). In this case, d_N is the number of nonsynonymous substitutions per nonsynonymous site, and d_S is the number of synonymous substitutions per synonymous site.

Accession numbers

The Fd sequence data from UWO241 have been deposited in GenBank (see Table 2, later).

Results

Characterization of Fd from algal cultures

Ferredoxin could be detected in the soluble protein extract of both UWO241 and *C. reinhardtii* (Fig. 1a,b), confirming that the antibody raised specifically against PETF from *C. reinhardtii* cross-reacts with Fd from UWO241. We confirmed the successful isolation and purification of Fd from both species. The final extracted proteins gave a single band on an SDS-PAGE and IEF with estimated purity of 98% based on densitometry measurements of the Commassie-stained gels (Fig. 1a,c). As with other plant-type Fds (Schmitter *et al.*, 1988), the electrophoretic migration of the algal Fds upon SDS-PAGE exhibited anomalies. Based on its primary amino acid sequence, the predicted molecular weight of PETF from *C. reinhardtii* is 9.91 kDa. However, this protein was detected at 22 kDa by SDS-PAGE. In comparison, Fd from UWO241 was detected as a 20 kDa polypeptide (Fig. 1a,b). The isoelectric points (pI) of Fd from *C. reinhardtii* and UWO241 were estimated using IEF of the purified proteins along a low pH range (Fig. 1c), as most plant-type Fds are rich in acidic residues (Fukuyama, 2004). Fd from the psychrophile UWO241 displayed lower pI (pI = 3.9) as compared with PETF from *C. reinhardtii* (pI = 4.0). The plant-type Fds in the oxidized state are typically reddish-brown in color as a result of the [2Fe-2S] cluster and exhibit a typical absorption maxima at 462, 422, 330, and 275 nm (Schmitter *et al.*, 1988; Fukuyama, 2004). We observed this typical absorption spectrum with both purified algal proteins, using a commercially available Fd from spinach as a control (Fig. 1d).

Antibody probing of soluble protein extracts revealed the presence of *c.* 3.1 times more Fd in UWO241 than in *C. reinhardtii* (Fig. 1a,b). UWO241 is halotolerant and can grow in salinities up to 700 mM NaCl (Takizawa *et al.*, 2009). To test whether salinity influences the accumulation of Fd in UWO241, we extracted total proteins from cultures grown in low- and high-salt media. Once again, we observed higher Fd protein accumulation in the psychrophile than in the mesophile; however, there were no observable differences in the amount of Fd in UWO241 grown at different salinities (Figs 1e,f, S2).

The sequence and structure of psychrophilic Fd-1

We determined the amino acid sequence of purified Fd from UWO241 using MS and detected the presence of two highly similar proteins in the same fraction (Fd-1A and Fd-1B; Table S1). A BLAST search confirmed that both proteins were closely related to photosynthetic Fd sequences from green algae and plants. Sequencing of purified Fd from *C. reinhardtii* identified a single protein with 100% identity with the known *C. reinhardtii* PETF sequence (not shown).

To examine key features present in the Fd primary protein sequences from UWO241, we performed multiple sequence comparison with Fds from a variety of photosynthetic species (Fig. 2). All Fds examined were 94–96 amino acids long, and highly conserved at the primary protein sequence (90.4–62.8% identity compared with Fd from UWO241), even among evolutionarily distant lineages. Each Fd, including Fd-1A and Fd-1B from UWO241, contained the conserved $CX_4CX_2CX_nC$ motif involved in coordination of the [2Fe-2S] cluster (Fukuyama, 2004; Hanke & Mulo, 2013). The region around the metal binding site (particularly the 35–51 loop containing the first three cysteines) showed the highest conservation among all species (Fig. 2;

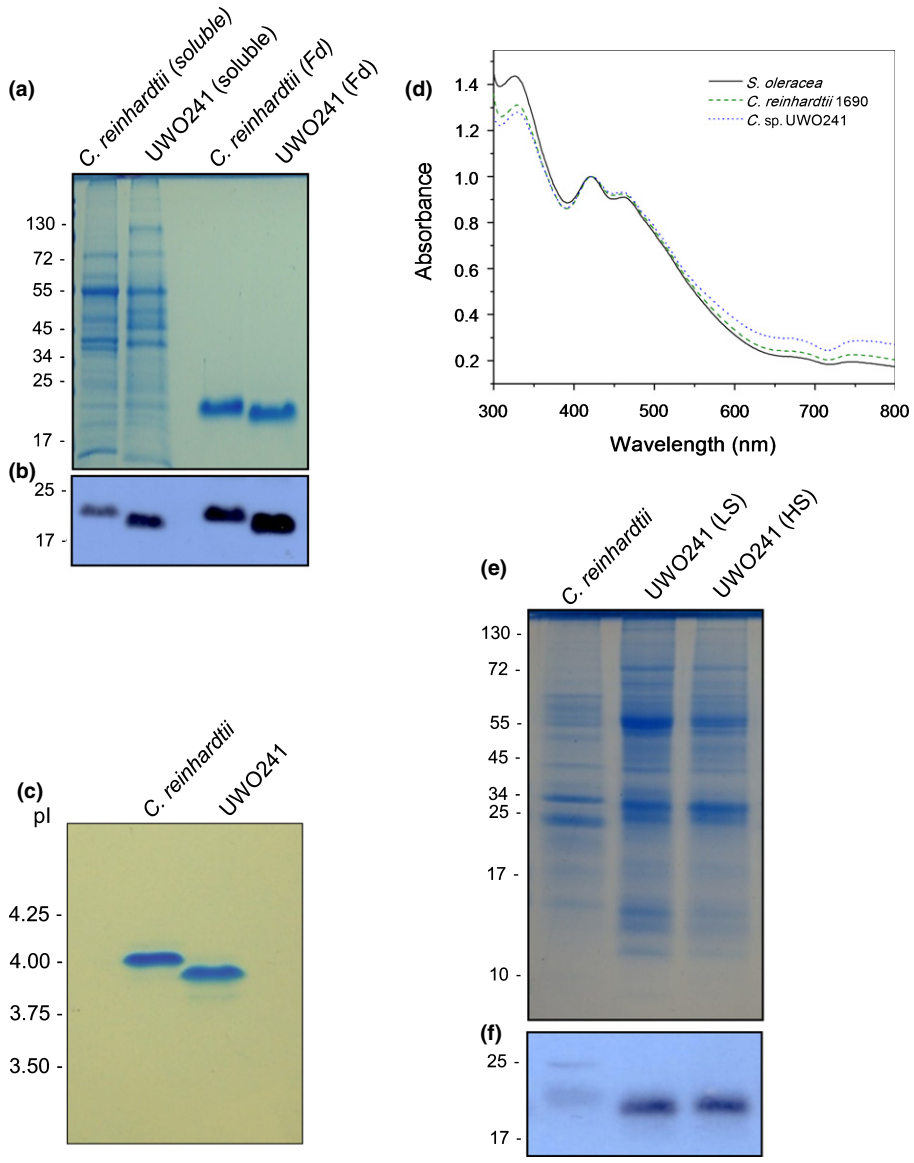

Fig. 1 (a) Coomassie-stained sodium dodecyl sulfate-polyacrylamide gel electrophoresis (SDS-PAGE) gel of soluble proteins from *Chlamydomonas reinhardtii* and *Chlamydomonas* sp. UWO241 (lanes 1 and 2), and purified ferredoxin (Fd) from *C. reinhardtii* and UWO241 (lanes 3 and 4). (b) Corresponding immunoblot of soluble proteins and purified Fd using antibodies specific for Fd. Molecular mass (kDa) is indicated on the left. (c) Isoelectric focusing of purified Fd from *C. reinhardii* and UWO241 along a narrow pH range (3–5). Isoelectric point (pI) values are indicated on the left. (d) Light absorption spectra of purified Fd from *C. reinhardtii* and UWO241, and commercially available pure Fd from *Spinacia oleracea*, measured at 300–800 nm. All measurements were performed at room temperature. (e) Coomassie-stained SDS-PAGE gel of total proteins from *C. reinhardtii* (lane 1) and UWO241 grown in 70 mM (low salt (LS); lane 2) and 700 mM (high salt (HS); lane 3) NaCl. (f) Corresponding immunoblot of total proteins probed with antibodies specific for Fd-1.

Bertini *et al.*, 2002). Fd transfers electrons from PSI to several target enzymes through the formation of electron transfer protein complexes predominantly by electrostatic interactions. All residues implicated in the interactions of Fd with various enzymatic partners (Akashi *et al.*, 1999; García-Sánchez *et al.*, 2000; Kurisu *et al.*, 2001; Hanke *et al.*, 2004b; Maeda *et al.*, 2005; Saitoh *et al.*, 2006; Chang *et al.*, 2007; Winkler *et al.*, 2009; Sakakibara *et al.*, 2012; Rumpel *et al.*, 2015) were conserved in the psychrophile UWO241 (Fig. 2). Based on the amino acid sequence, Fd-1A and Fd-1B have predicted molecular masses of 9.80 and 9.86 kDa, respectively.

When aligned, the amino acid sequences of the two Fd isoforms from UWO241 and PETF from *C. reinhardtii* differ at 11 sites (Fig. 2). These residues are in regions of the protein that are highly variable even among closely related species. These differences do not change the protein charge (i.e. an overall negative charge is maintained); however, they do alter hydrophobicity, potentially affecting the physical properties of the protein. Both Fd-1A and Fd-1B from UWO241 have more hydrophilic (polar) residues when compared with PETF (Table 1). We predicted and compared the tertiary structures of the psychrophilic and mesophilic Fd proteins studied here (Fig. 3). Our results show

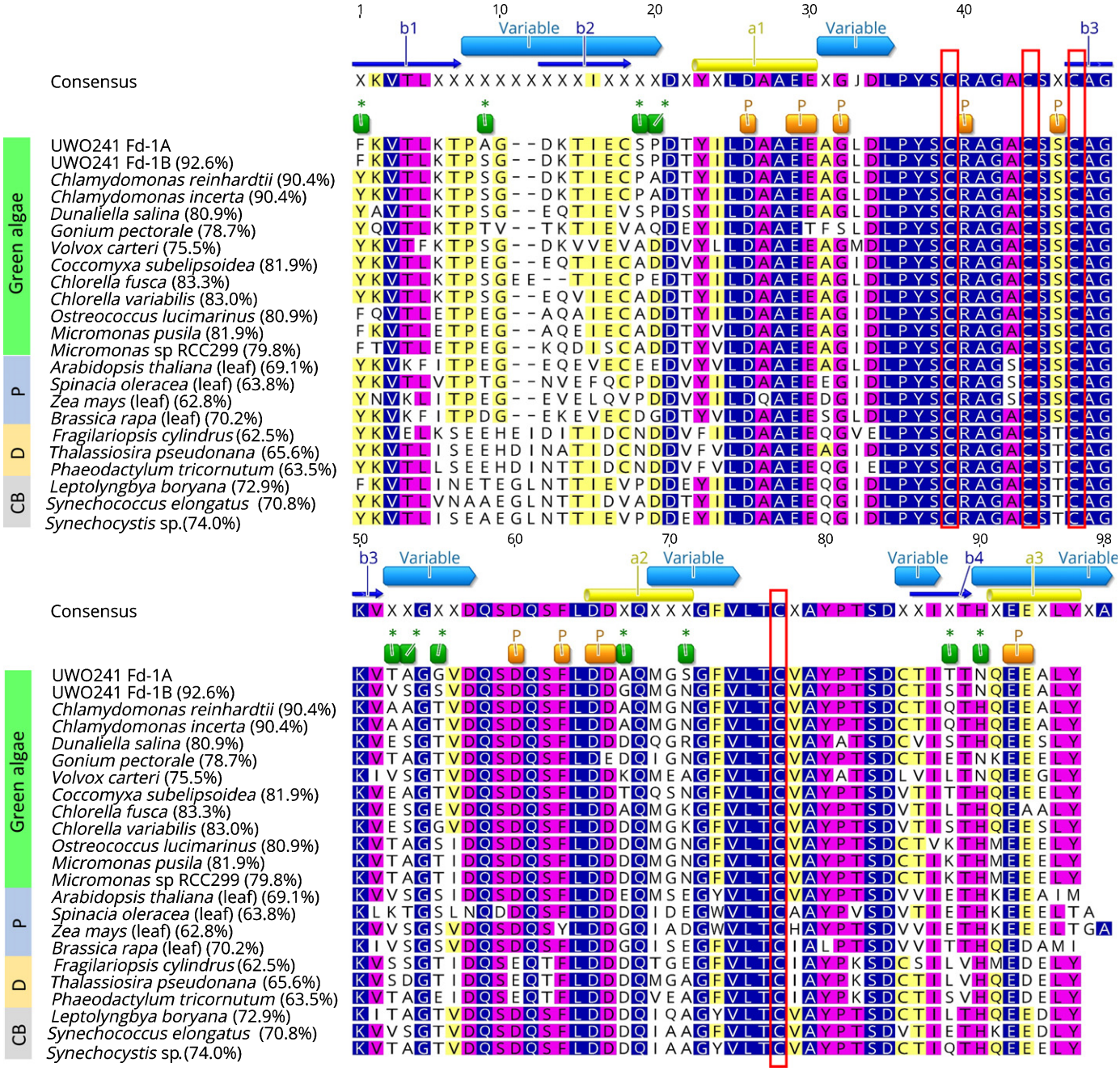

Fig. 2 Alignment of photosynthetic ferredoxin (Fd) proteins from *Chlamydomonas* sp. UWO241 with that of green algae, plants (P), diatoms (D), and cyanobacteria (CB), using the ClustalW algorithm (Sievers *et al.*, 2011). Only the active Fd proteins lacking the chloroplast signal peptide are shown. The color of the residue depends on the degree of conservation among species (blue, fully conserved; purple, 80–100% similar; yellow, 60–80% similar; white, < 60% similar). The consensus sequence (75% similarity between all sequences) is shown above the alignment and annotated to indicate the presence of α-helices (1–3), β-sheets (1–4) and the variable regions (as determined by Bertini *et al.*, 2002; Kameda *et al.*, 2011). The percentage identity to Fd-1A from UWO241 is indicated in parentheses next to the species name. The highly conserved cysteine residues involved in coordinating the [2Fe-2S] cluster are marked with a red box (Cys39, Cys44, Cys47, Cys77). Residues involved in protein–protein interaction of Fd and its partners (Asp26, Glu29, Glu30, Gly32, Arg40, Ser46, Asp60, Phe63, Asp65, Asp66, Glu92, Glu93) are indicated with an orange square (P). Residues which are different between the two Fd proteins from UWO241 and PETF from *C. reinhardtii* are indicated with a green square (*). See Results section for more details.

that the structures of these enzymes are highly similar to previously determined and modeled structures of other photosynthetic Fds (Figs 3, S3). The psychrophilic and mesophilic proteins showed a high degree of overlap between models, with several minor differences in the loop regions. For instance, the loop containing residues Pro19 and Ala20 in the mesophilic PETF had a different conformation in the psychrophilic Fds where these residues are substituted with Ser19 and Pro20 (Fig. 3).

We also performed a phylogenetic analysis of Fds from various species, using a structure-based alignment, to determine if the

Table 1 A list of the amino acid (AA) substitutions in the sequences of the active ferredoxin (Fd) enzymes from *Chlamydomonas reinhardtii* and UWO241, comparing the hydropathy and charge between the substituted residues

	C. reinhardtii Fd-1				UWO241 Fd-1A				UWO241 Fd-1B			
Position	Codon	AA	Hydropathy	Charge	Codon	AA	Hydropathy	Charge	Codon	AA	Hydropathy	Charge
1	TAC	Tyr	Hydrophobic	N	TTC	Phe	Hydrophobic	N	TTC	Phe	Hydrophobic	N
9	TCG	Ser	Hydrophilic (polar)	N	GCC	Ala	Hydrophobic	N	TCA	Ser	Hydrophilic (polar)	N
19	CCC	Pro	Hydrophobic	N	TCC	Ser	Hydrophilic (polar)	N	TCC	Ser	Hydrophilic (polar)	N
20	GCT	Ala	Hydrophobic	N	CCG	Pro	Hydrophobic	N	CCG	Pro	Hydrophobic	N
53	GCT	Ala	Hydrophobic	N	ACT	Thr	Hydrophilic (polar)	N	GTC	Val	Hydrophobic	N
54	GCC	Ala	Hydrophobic	N	GCC	Ala	Hydrophobic	N	TCG	Ser	Hydrophilic (polar)	N
56	ACC	Thr	Hydrophilic (polar)	N	GGC	Gly	Hydrophobic	N	TCC	Ser	Hydrophilic (polar)	N
67	GCC	Ala	Hydrophobic	N	GCG	Ala	Hydrophobic	N	GGC	Gly	Hydrophobic	N
71	AAC	Asn	Hydrophilic (polar)	N	TCC	Ser	Hydrophilic (polar)	N	AAC	Asn	Hydrophilic (polar)	N
88	CAG	Gln	Hydrophilic (polar)	N	ACC	Thr	Hydrophilic (polar)	N	TCC	Ser	Hydrophilic (polar)	N
90	CAC	His	Moderate	+	AAC	Asn	Hydrophilic (polar)	N	AAC	Asn	Hydrophilic (polar)	N

The hydrophilic residues are highlighted in gray, while the hydrophobic residues are in white. The position of the residues is based on the multiple sequence alignment in Fig. 2.

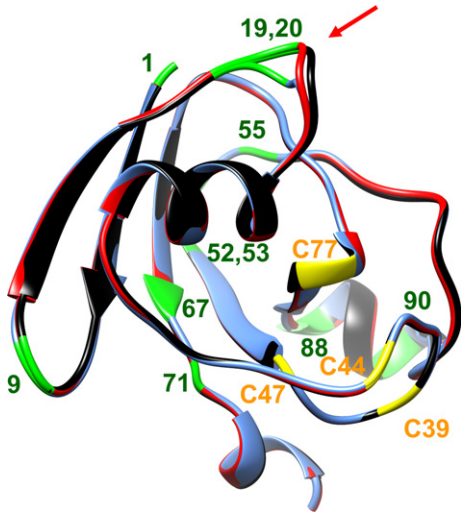

Fig. 3 Predicted tertiary structure of the two ferredoxin (Fd) isoforms from *Chlamydomonas* sp. UWO241 (Fd-1A in red; Fd-1B in black) superimposed on the structure of photosynthetic Fd (PETF) from *Chlamydomonas reinhardtii* (blue). The structure of *C. reinhardtii* PETF was obtained from PDB (ID: 2mh7). Fd-1A and Fd-1B were modeled based on homologous proteins using the PHYRE^2 Engine (Kelley *et al.*, 2015). The positions of the conserved cysteine residues involved in coordination of the [2Fe-2S] cluster are labeled and highlighted in yellow. The residues that are different between sequences are labeled and highlighted in green. The regions where the structure of the proteins is most different is indicated by a red arrow. The residue number corresponds to the sequence alignment shown in Fig. 2. Molecular graphics and analyses were performed with UCSF Chimera (Pettersen *et al.*, 2004).

psychrophilic Fds from UWO241 are structurally more similar to Fds from other cold-adapted species, such as the trebouxiophyceaen *Coccomyxa subelipsoidea* and the diatom *Fragilariopsis cylindrus* (Fig. 4). Our analysis showed that Fd-1A and Fd-1B from UWO241 are more similar to homologs from closely related mesophilic species than to more distantly related cold-adapted organisms.

To examine if Fd enzymes from UWO241 are under evolutionary pressure to gain cold-adapted characteristics, we calculated the $d_N : d_S$ (ω) ratio, that provides a measure of selective pressure at the amino acid level (Yang & Bielawski, 2000). Both Fd-1A and Fd-B had a value of $\omega < 1$ when compared with PETF from *C. reinhardtii*, suggesting that these proteins are under purifying selection that favours sequence conservation ($\omega = 0.19$, $d_N = 0.14$, $d_S = 0.77$, comparing Fd-1A and PETF; $\omega = 0.24$, $d_N = 0.17$, $d_S = 0.68$, comparing Fd-1B and PETF). Overall, our analyses suggest that the psychrophilic Fd proteins from UWO241 are under strong evolutionary pressure to conserve their primary amino acid sequence and thus retain the main functions common to all plant-type Fds.

Transcriptomic and genomic analysis of UWO241 ferredoxins

Our results suggest that UWO241 accumulates two highly similar Fd-1 proteins. By screening the UWO241 genome and transcriptome, we confirmed the presence of two Fd-1 genes at both the DNA and RNA levels. This differs from *PETF* from *C. reinhardtii*, which is encoded by a single gene (Terauchi *et al.*, 2009). Both *Fd* transcripts from UWO241 were present in the transcriptomic data at high levels: the average coverages per nucleotide were 9978× and 15 925×, respectively (as determined by aligning the RNAseq reads to the full transcript sequence of each gene), suggesting that both genes were expressed under the growth conditions used in this study.

At the genome level, Fd-1A and Fd-1B differ in gene structure (Fig. 5), with the noncoding regions sharing 54% identity and the coding regions sharing 91% identity. Both genes have a length of 1114 bp (three introns, four exons). In comparison, the *PETF* gene from *C. reinhardtii* is 593 bp (one intron, two exons). The difference in gene length between species is a result of a higher noncoding content in the genes from UWO241. The protein-coding sequences were similar in length between species; however, in both *Fd-1A* and *Fd-1B* from UWO241, only 33% of

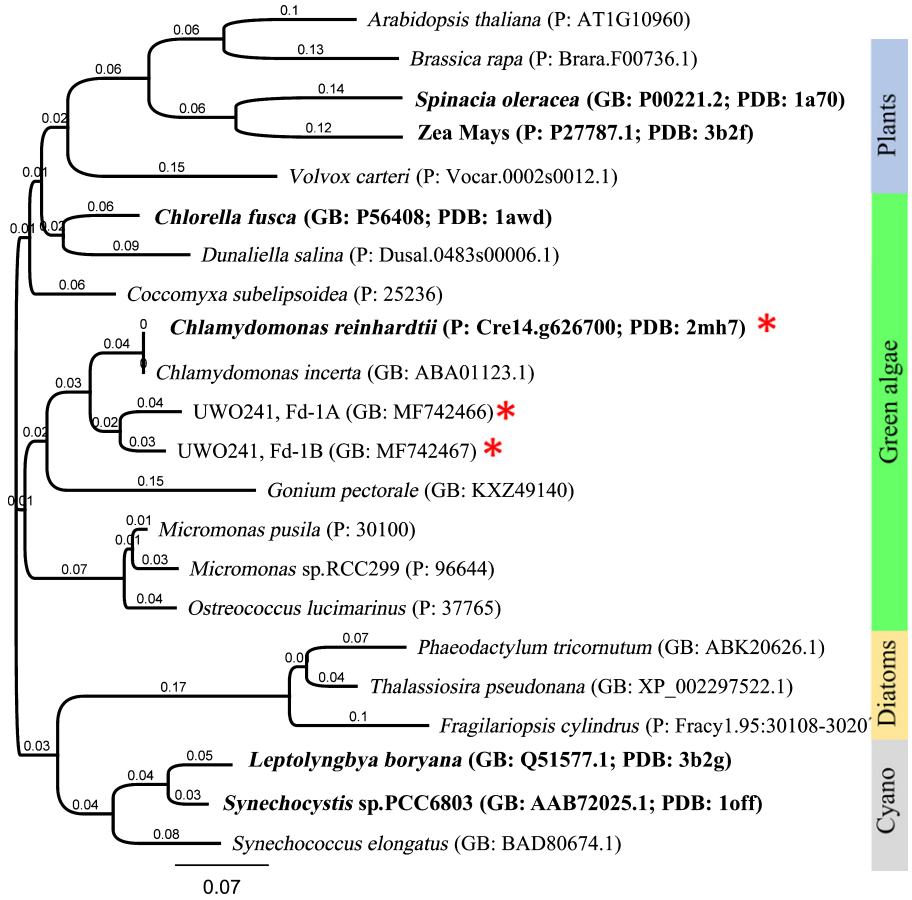

Fig. 4 Molecular phylogenetic analysis of photosynthetic ferredoxin (Fd-1/PETF) of various green algae, higher plants, diatom and cyanobacterial species by a maximum likelihood method. The sequences used in the analysis were obtained from GenBank (GB) or Phytozome (P). The phylogenetic tree is based on the active ferredoxin (Fd) amino acid sequences lacking a chloroplast transition peptide (94 aa). A structure-based alignment was first created using the MATT algorithm (Menke *et al.*, 2008) with known structural coordinates, where known (PDB ID, bold). This alignment was used to map the relationships of Fd sequences without solved structures using the MUSCLE algorithm (Edgar, 2004). The tree is represented to scale with branch lengths measuring the number of substitutions per site. The position of the sequences from the two species studied here, *Chlamydomonas* sp. UWO241 and *Chlamydomonas reinhardtii*, are indicated with a red asterisk.

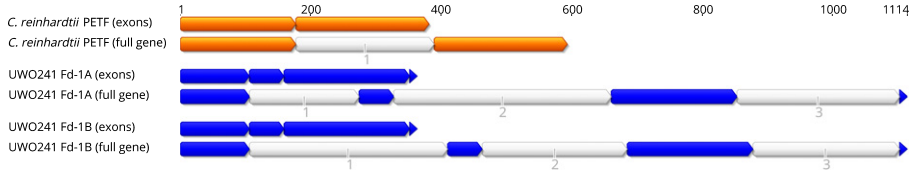

Fig. 5 A graphical representation of the gene structure of photosynthetic ferredoxin genes in the psychrophile *Chlamydomonas* sp. UWO241 and the mesophile *Chlamydomonas reinhardtii*. In all cases, the noncoding intron sequences are shown in white and sequentially numbered, while the protein-coding exon sequences are shown in color (orange for *C. reinhardtii*, and blue for UWO241). Both the full gene and the concatenated exonic sequences are shown, demonstrating the difference in gene structure between the two organisms.

the full gene length was exonic, while in *PETF* from *C. reinhardtii*, 64% of the full gene length was exonic. These results suggest that the gene encoding for Fd-1 has undergone a recent duplication event in UWO241, with selective pressure operating at the level of the protein – thus, the coding DNA sequences remain similar.

Green algae and plants contain multiple Fd isoforms, which have different functions (Winkler *et al.*, 2010; Peden *et al.*, 2013; Sawyer & Winkler, 2017). We screened the UWO241 genome and identified eight genes encoding putative Fds (Table 2). Of these, Fd-1A and Fd-1B were most similar (90.8% identity at the amino acid level), while the rest of the Fd sequences were more divergent, displaying a low amino acid sequence identity (Fig. S4). All UWO241 Fds were predicted to contain the [2Fe-2S] binding domain and clustered within previously defined classes in green algae (Yang *et al.*, 2015; Sawyer & Winkler, 2017) and plants (Fukuyama, 2004; Atkinson *et al.*, 2016) (Fig. 6). Six of these sequences (Fd-1A, Fd-1B, Fd-3, Fd-4, Fd-6,

Fd-7) were identified as plant-type Fds based on the presence of the highly conserved $CX_4CX_2CX_nC$ motif. Fd-11 and mFd contained the motif $CX_5CX_2CX_nC$, which is typical for nonphotosynthetic adrenodoxins that are involved in mitochondrial metabolism (Ewen *et al.*, 2012). All Fds were predicted to localize to the chloroplast, except for mFd which was predicted to localize to the mitochondrion. The Fd genes from UWO241 had a higher average noncoding DNA content (70.5%) as compared with Fd genes from *C. reinhardtii* (48.7%).

Effects of temperature on Fd-1 stability and activity

Enzymes from cold-adapted organisms often display high activity at low temperatures accompanied by decreased thermostability at higher temperatures (Feller & Gerday, 2003). To test whether this is the case for Fd, we measured the change in protein conformation across a temperature range (5–80°C). We showed that Fds from both algal species undergo conformational changes with increasing temperature. PETF from *C. reinhardtii* reached its final unfolded state at 65°C (Fig. 7a), whereas Fd from UWO241 exhibited a more gradual unfolding with increasing temperature, reaching its final conformation at 60°C (Fig. 7b). The loss of secondary structural elements, such as α-helices and β-sheets, can be followed by observing the change in protein ellipticity at a specific wavelength (Greenfield, 2006). The losses of α-helices in Fd proteins from both algae werecomparable up to 45°C; however, at higher temperatures the psychrophilic Fd from UWO241 lost its α-helical structure more rapidly and unfolded completely at temperatures ≥ 60°C (Fig. 7c). By contrast, mesophilic PETF unfolded only partially at temperatures ≥ 65°C, suggesting that this protein retains considerable α-helical content in a 'molten globule state' (Kuwajima, 1989). Both proteins fully lost their β-sheet content (Fig. 7d), but this happened at lower temperatures for the psychrophilic Fd (> 60°C) than for the mesophilic PETF (> 70°C). To confirm that this effect is specifically due to temperature, we measured the change in secondary structures in response to the chemical denaturant Gn-HCl. In this case, Fd from both algal species showed similar conformational changes at the level of the full protein (Fig. 8a,b) and secondary structures (Fig. 8c,d). We conclude that the structure of Fd from the psychrophilic alga is specifically more sensitive to increases in temperature than is the structure of Fd from the mesophilic alga.

To complement the structural stability of Fd, we also measured the temperature dependence of *in vitro* Fd activity over a temperature range of 5–70°C. The temperature profile for Fd activity for UWO241 peaked at 10°C and decreased gradually to a value of zero at 70°C. By contrast, the activity of PETF from *C. reinhardtii* was threefold lower at 10°C than Fd from UWO241, maximum at 40°C and minimal at 70°C (Fig. 9a). Fd activity for the psychrophile and mesophile were comparable at 60°C. This temperature profile for Fd activity was complemented by an examination of the time-dependence for the stability of enzyme activity at 10, 40 and 60°C (Fig. 9b–d). As expected for cold-adapted proteins, Fd from UWO241 maintained high initial activity at 10°C which increased by 40–50% with prolonged incubation at this temperature (Fig. 9b). By contrast, PETF from *C. reinhardtii* exhibited a 50% inhibition in activity during the first 30 min of incubation at 10°C (Fig. 9b). We note that both proteins retained their secondary structure during incubation at this temperature, as determined by CD spectroscopy (Fig. S5a,b). We discovered that incubation of Fd from both species at 40°C stimulated enzyme activity by about twofold, with minimal change in their conformation over time (Figs 9c, S5c,d). Finally, both enzymes showed an inhibition of Fd activity at 60°C. However, after 1 h at 60°C, no activity was detected for UWO241 Fd, while *C. reinhardtii* PETF retained close to 60% of its activity (Fig. 9d). Protein ellipticity revealed that at this temperature, Fd from UWO241 reached its final conformational state within 5 min of exposure to 60°C, while that from *C. reinhardtii* exhibited a more gradual, time-dependent conformational change at this temperature (Fig. S5e,f). We conclude that psychrophilic Fd from UWO241 is structurally and functionally adapted specifically to function at cold temperatures.

Table 2 Ferredoxin (Fd) genes present in the genome of UWO241

Gene[a]	GenBank	Localization[b]	*Chlamydomonas reinhardtii* homolog (% identity)	Gene			Protein[c]		
				Length (bp)	Introns	Noncoding (%)	Length (aa)	MW (kDa)	pI
Fd-1A	MF742466	Chloroplast	PETF/Fd-1 (75.2%)	1114	3	67.41	120.00	12.62	4.56
Fd-1B	MF742467	Chloroplast	PETF/Fd-1 (77.2%)	1114	3	67.41	120.00	12.61	4.56
Fd-3	MG748623	Chloroplast	FDX3 (53.3%)	890	2	40.34	176.00	19.10	5.38
Fd-4	MG748624	Chloroplast	FDX4 (63.6%)	1979	3	80.90	125.00	13.51	6.08
Fd-6	MG748625	Chloroplast	FDX6 (56.7%)	4072	5	76.42	319.00	34.05	4.55
Fd-7	MG748626	Chloroplast	FDX7 (28.8%)	1493	3	73.88	129.00	13.01	4.30
Fd-11	MG748628	Chloroplast	FDX11 (44.8%)	2411	5	83.20	134.00	14.36	8.04
mFDX	MG748627	Mitochondria	MFDX (55.9%)	2358	4	75.06	195.00	20.64	5.06

Sequences were obtained by screening the genome using BLAST searches with known Fd sequences from *C. reinhardtii*, and other related algae and plant species. The genome was also screened using the most conserved regions of the Fd sequences, as determined by multiple-alignment analysis. aa, amino acids; pI, isoelectric points; MW, molecular weight.

[a]Ferredoxin genes from UWO241 were named based on the most closely related homolog from *C. reinhardtii*.

[b]Localization was predicted using the PREDALGO software.

[c]Protein length, MW and pI were predicted based on the gene coding sequence using the GENEIOUS software suite.

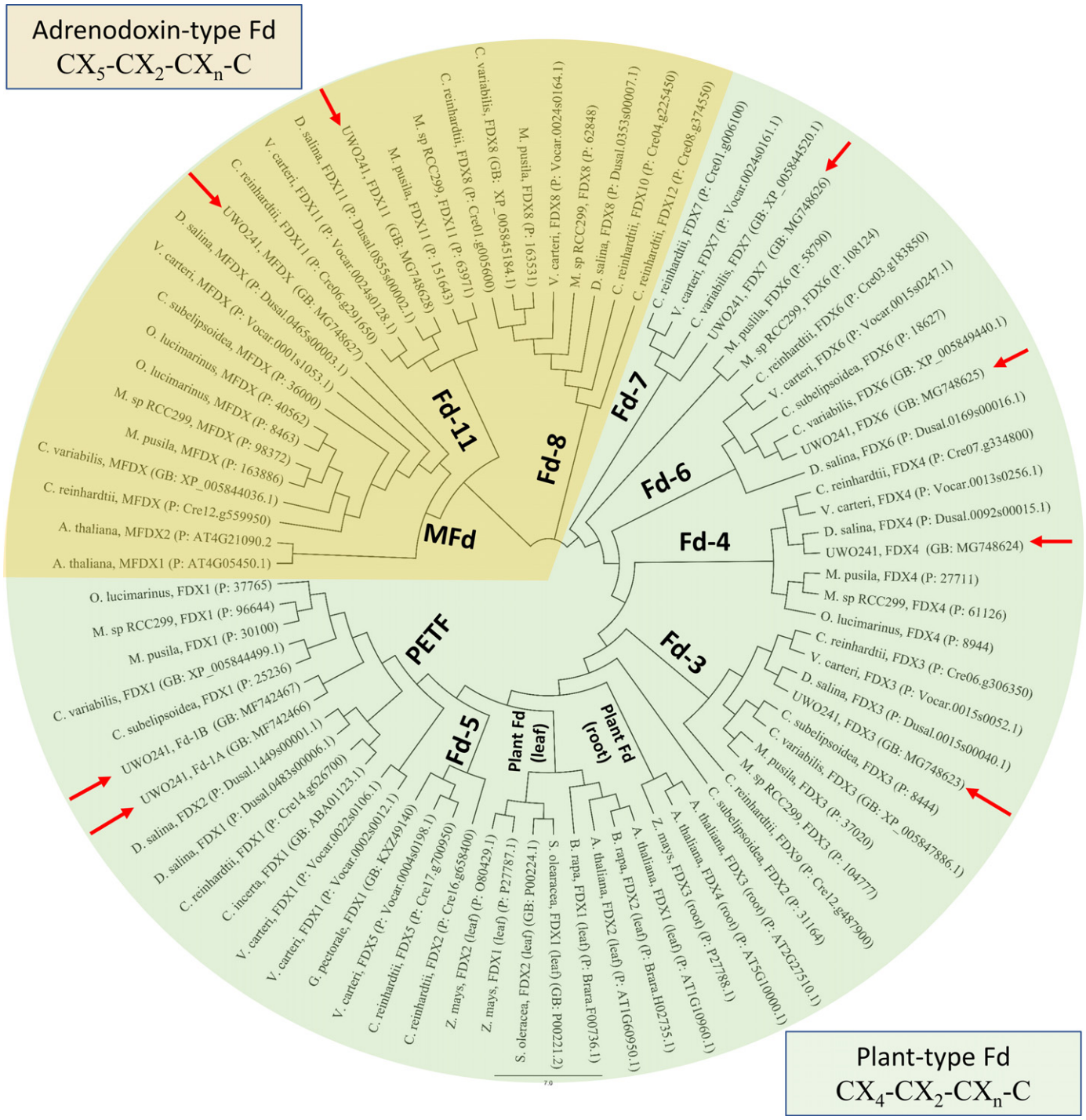

Fig. 6 Molecular phylogenetic analysis placing the ferredoxin (Fd) sequences from *Chlamydomonas* sp. UWO241 within defined Fd classes in related plants and green algae. The analysis is based on the full Fd amino acid sequences, analyzed by multiple sequence alignment to map the relationships of the novel psychrophilic Fd proteins to already defined Fd groups. The Fd groups shown here are based on sequence similarity with characterized members of the Fd gene family from *Chlamydomonas reinhardtii* (for algae) and *Arabidopsis thaliana* (for plants). The sequences used in the analysis were obtained from GenBank (GB) or Phytozome (P), and the associated accession numbers are shown in parentheses next to the species name. The position of the Fd sequences from UWO241 are indicated with a red arrow.

Although Fd from UWO241 is more sensitive to increases in incubation temperature tha is Fd from *C. reinhardtii*, it also exhibits an unusual property of retaining high activity and structural stability at moderate temperature temperatures (40°C).

Discussion

Ferredoxin from the psychrophilic alga UWO241 is specifically adapted to function in the cold. Psychrophilic Fd-1 has higher

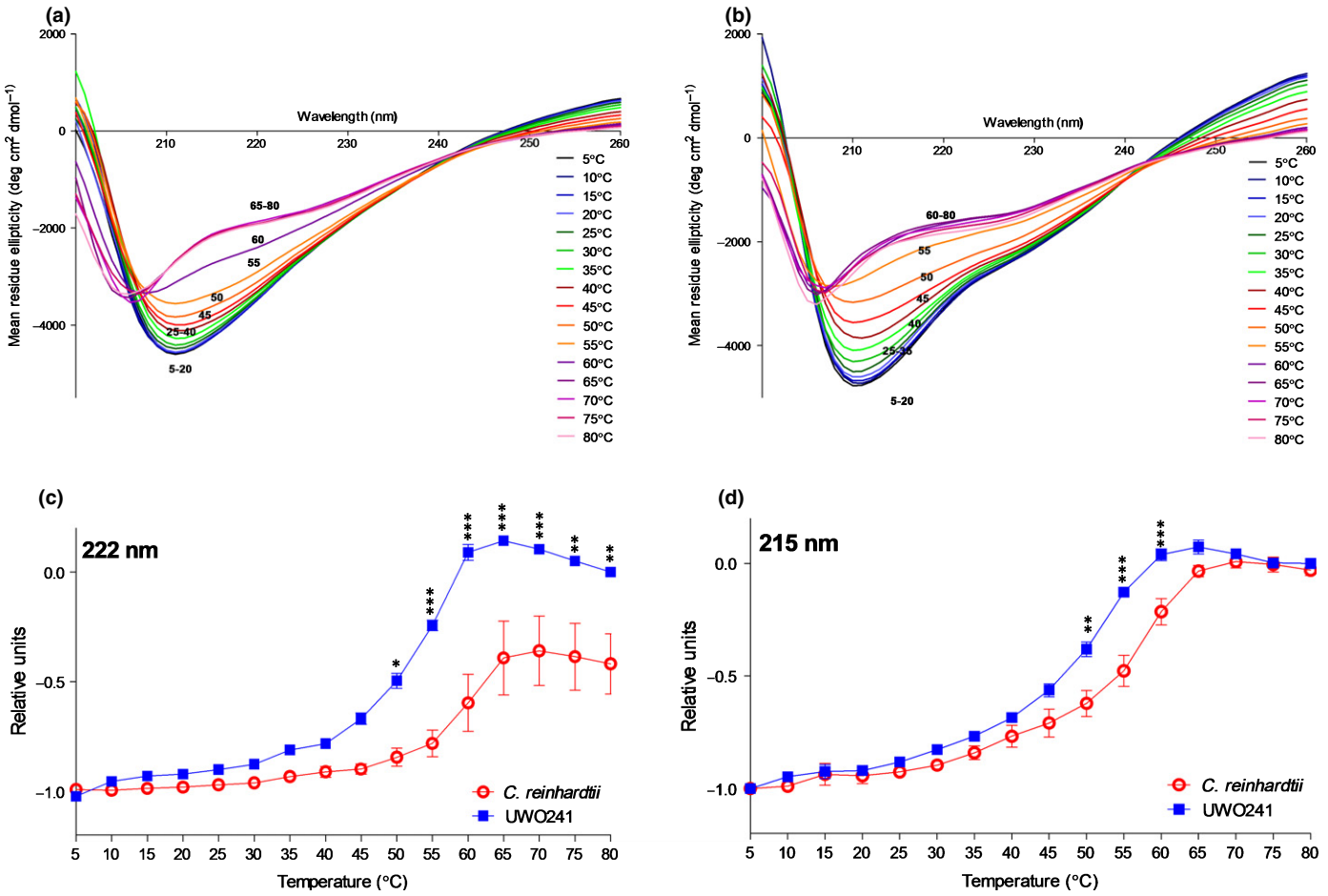

Fig. 7 The change in secondary structure of purified photosynthetic ferredoxin (Fd) from (a) *Chlamydomonas reinhardtii* and (b) *Chlamydomonas* sp. UWO241 as a function of changing temperature, measured by circular dichroism spectroscopy (representative experiments). The mean residue ellipticity at 222 nm (c), corresponding to α-helix structure, and at 215 nm (d), corresponding to β-sheet structure, were plotted against temperature. The *y*-axis represents the protein folding state, with –1 corresponding to completely folded protein and 0 corresponding to completely unfolded protein. Data are means ± SE of three independent experiments. Data were analyzed by two-way ANOVA followed by a Bonferroni post-test to compare the change of Fd structure with temperature between the two algal species. Statistical significance: *, $P < 0.05$; **, $P < 0.01$; ***, $P < 0.001$.

activity at 10°C and is more thermolabile at 60°C than mesophilic PETF from *C. reinhardtii*. Interestingly, psychrophilic Fd maintains high activity at moderate temperatures (40°C), which are generally prohibitive to the functioning of most psychrophilic enzymes (Feller & Gerday, 2003; Collins *et al.*, 2008). There are only a few studies that have specifically explored the cold adaptation of green algal proteins. For instance, nitrate reductase and glucose-6-phosphate dehydrogenase were shown to have typical cold-adapted characteristics in several psychrophilic algal species, including the chlamydomonadalean *Chloromonas* spp. (Loppes *et al.*, 1996) and *Koliella antarctica* (Vona *et al.*, 2004; Di Martino *et al.*, 2006; Ferrara *et al.*, 2013). Not all enzymes from cold-adapted algae exhibit high activity in the cold and thermal instability at warmer temperatures. For example, psychrophilic ribulose-1,6-biphosphate carboxylase (RuBisCo) has low activity at cold temperatures, but the cellular concentrations of this enzyme in polar algae were twice as high as in mesophilic algae (Devos *et al.*, 1998). UWO241 also accumulates higher concentrations of the large subunit of RuBisCo, as compared with a related mesophile (Dolhi *et al.*, 2013). Thus, we suggest that cold-adapted algae have two strategies to overcome the restrictions of cold temperatures on their enzyme activity: adaptations in the protein primary amino acid sequence that lead to significant increases in activity at low temperature; and biosynthesis of large quantities of key proteins to provide enough enzymatic activity to power important cellular process. We propose that Fd-1 from UWO241 is unique among algal psychrophilic proteins explored to date, in that it exhibits characteristics specific to both strategies, namely high activity at 10°C and higher protein amounts.

A novel feature of UWO241 is the expression and accumulation of two Fd-1 isoforms that exhibit discrete differences in the amino acid sequence. We propose that these amino acid substitutions result in the observed increase in cold activity observed for Fd-1 from UWO241. The molecular origin(s) of enzyme cold activity associated with psychrophily has been difficult to pinpoint accurately and there are no known sequence or structural elements that can be used to predict whether an enzyme is cold-adapted. An overarching observation from comparing the amino acid sequences and crystal structure, where available, between

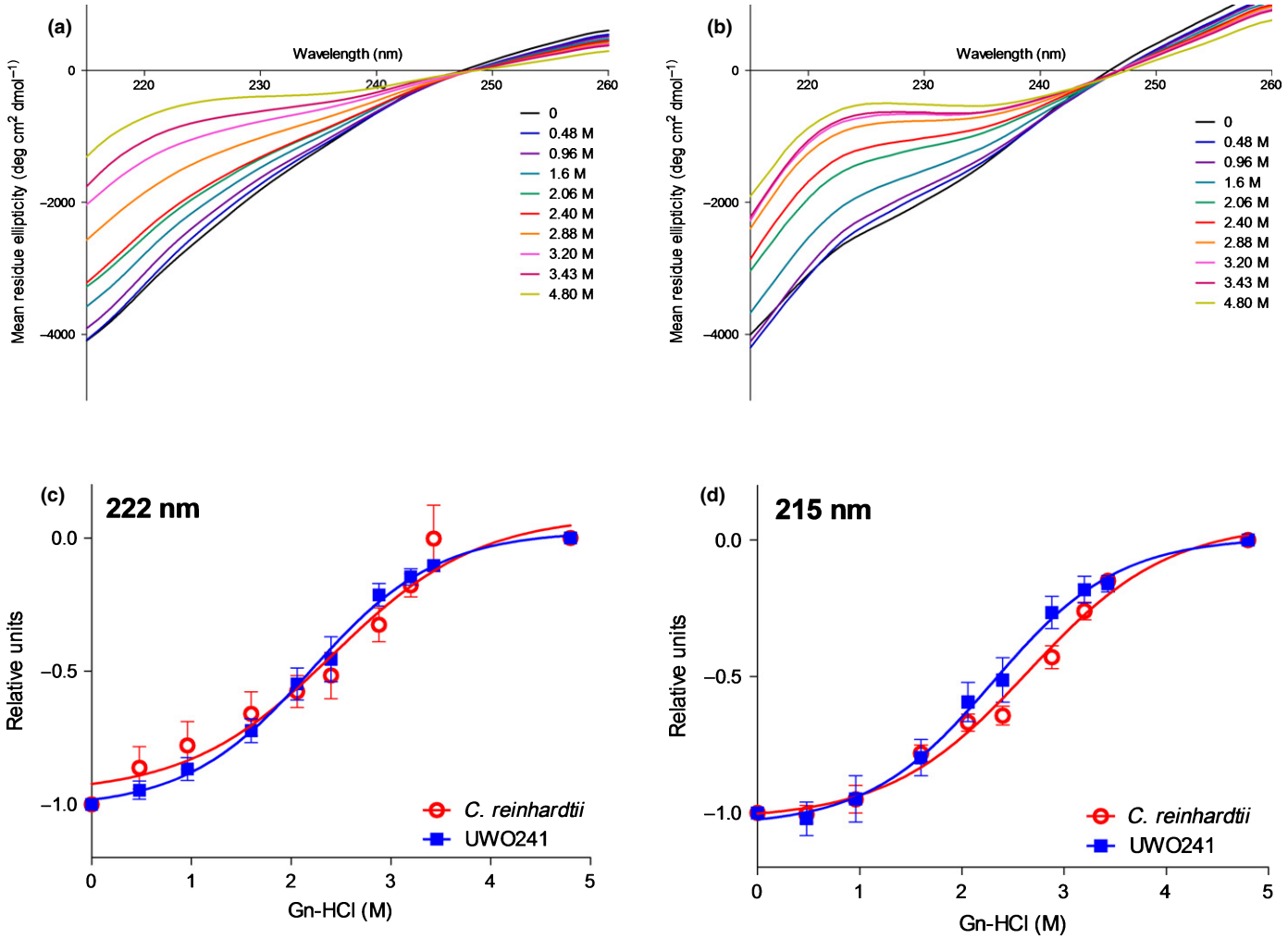

Fig. 8 The change in secondary structure of purified photosynthetic ferredoxin (Fd) from *Chlamydomonas reinhardtii* (a) and *Chlamydomonas* sp. UWO241 (b) as a function of chemical denaturation by adding Gn-HCl, measured by circular dichroism spectroscopy (representative experiments). Nonlinear fit analysis of the mean residue elipticity at 222 nm (c), corresponding to α-helix structure, and at 215 nm (d), corresponding to β-sheet structure, plotted against Gn-HCl concentration. The *y*-axis represents the protein folding state, with −1 corresponding to completely folded protein and 0 corresponding to completely unfolded protein. Data are the means ± SE of three independent experiments. Data were analyzed by two-way ANOVA followed by a Bonferroni post-test to compare the activity of Fd with changing temperature between the two algal species, with no significant differences found.

psychrophilic proteins and their mesophilic counterparts is that orthologous enzymes often show a high degree of sequence and structural similarity. Furthermore, amino acids that are part of the catalytic site are typically strictly conserved. Consequently, changes occurring at positions other than the enzyme active site are likely to be responsible for the improved protein dynamics (Aghajari *et al.*, 1998; D'Amico *et al.*, 2003; Åqvist *et al.*, 2017). We see a similar trend in our results. The residues that are different between the mesophilic and psychrophilic Fd-1 are in regions of the proteins that are distant from the active sites involved in metal binding or protein–protein interactions. Thus, the higher Fd cold activity in UWO241 is probably a result of individual substitutions that change the conformation in the loop regions of the proteins (such as residues in position 19 and 20; Fig. 2), or changes in the overall hydrophobicity of the psychrophilic proteins (Table 1). These relatively minor differences can nevertheless lead to significant increases in activity at low temperatures. In fact, there are several examples of psychrophilic proteins, such as bacterial subtilisin (Narinx *et al.*, 1997), triose phosphate isomerase (Alvarez *et al.*, 1998), and α-glucosidase (Noguchi *et al.*, 2009), where a single amino acid substitution provides improved cold activity.

Our results reveal the presence of two highly similar Fd-1 isoforms in the psychrophile UWO241, suggesting that the photosynthetic Fd gene has undergone a duplication event. The homologous Fd in other green algae and plants examined to date is encoded by a single gene. Fd-1A and Fd-1B are 92.6% identical, differing by only seven residues. We show that PETF from *C. reinhardtii* shares a higher sequence similarity with Fd-1A and Fd-1B from UWO241 (90%; Fig. 2) than with the other *C. reinhardtii* isoforms, confirming that both Fds from UWO241 are homologs of PETF. The genes encoding the Fd-

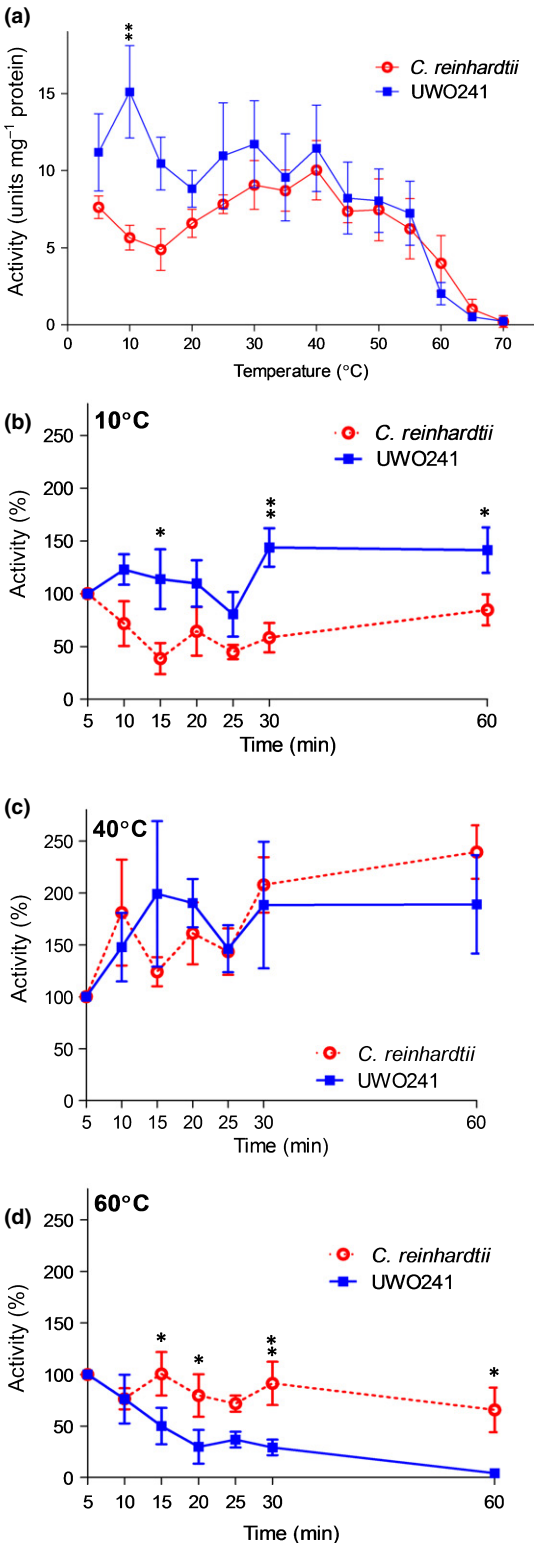

Fig. 9 Effects of temperature on the activity of purified photosynthetic ferredoxin (Fd) from *Chlamydomonas reinhardtii* (open red circles) and *Chlamydomonas* sp. UWO241 (closed blue squares). (a) In the first experiment, purified photosynthetic Fds were incubated at the appropriate temperature for 5 min, followed by measurement of their activity. The data are the means ± SE of four independent experiments. In the second set of experiments, activity of purified photosynthetic Fd from *C. reinhardtii* and UWO241 was measured after prolonged exposure to 10°C (b), 40°C (c), and 60°C (d). Results are expressed as a percentage of the starting activity measured at 5 min after the initial temperature exposure. The data are the means ± SE of three independent experiments. In all cases, data were analyzed by two-way ANOVA followed by a Bonferroni post-test to compare the activity of Fd with changing temperature between the two algal species. Statistical significance: *, $P < 0.05$; **, $P < 0.01$.

1A and Fd-1B proteins have similar architectures but are longer and have more exons and introns than the corresponding genes from other algae (Fig. S6). This suggests that the Fd-1 gene duplication in UWO241 is a relatively recent event, but enough time has gone by and enough mutations have accumulated that the intronic sequences from Fd-1A and Fd-1B are no longer alignable.

At the genome level, gene duplication is one of the main sources of functional diversity. Once duplicated, each gene copy can evolve independently and diversify its function (Lynch & Conery, 2000; Conant & Wolfe, 2008), which can be influenced not only by the specific role of the gene product but also by the amount of the gene product in the cell. For instance, multiple gene copies present in the genome can be linked to higher protein accumulation, a phenomenon known as gene dosage (Stranger *et al.*, 2007; Hahn, 2009; Innan & Kondrashov, 2010; Zhou *et al.*, 2011). Indeed, our data suggest that this is the case for Fd-1 in UWO241, and we provide evidence that the psychrophile accumulates higher amounts of Fd-1 (Fig. 1) than does the mesophile *C. reinhardtii*.

Large-scale studies that systematically test for positive selection regarding gene duplication are currently lacking, but there is a wealth of individual examples supporting the hypothesis that gene duplication is an adaptation to harsh conditions (Kondrashov, 2012). For example, gene duplication is important in the psychrophilic Antarctic cod, where duplication of important antifreeze proteins was 10 times more common in the psychrophile than in its mesophilic relatives (Chen *et al.*, 1997, 2008). Similarly, gene duplication increased the fitness of plants exposed to cold temperatures (Zhou *et al.*, 2009) and extreme salinities (Dassanayake *et al.*, 2011; Oh *et al.*, 2012), yeast under nutrient stress (Brown *et al.*, 1998), and bacteria exposed to heat (Christ & Chin, 2008) and heavy metal stress (von Rozycki and Nies, 2009; Yang *et al.*, 2010). It can be generalized that gene duplication as a form of adaptation to harsh environments is not a rare event, and it generally involves genes whose products need to be produced rapidly or constantly (Chen *et al.*, 2008; James *et al.*, 2008; DeBolt, 2010).

We hypothesize that higher amounts of photosynthetic Fd-1 in UWO241 are beneficial for life in the cold. In addition to its role in distributing photosynthetically derived reducing power, there is evidence that Fd-1 might be specifically associated with psychrophily. One of the most striking features of UWO241 is its inability to perform photosynthetic state transitions (Morgan-Kiss *et al.*, 2002; Szyszka *et al.*, 2007), which balance the energy distribution between PSI and PSII, and are the major mechanisms for achieving photostasis in green algae (Rochaix, 2014).

UWO241, however, has higher rates of CEF, specifically stimulated through a Fd-plastoquinone reductase-dependent pathway (Morgan-Kiss *et al.*, 2002). This pathway recycles photosynthetic electrons around PSI in order to maintain the redox poise of the cETC and prevent photodamage (Shikanai, 2007; Miyake, 2010). Consequently, it was suggested that CEF is the main mechanism for the regulation of energy balance in UWO241. CEF involves the transfer of electrons from Fd to the plastoquinone (PQ) pool through the protein PRGL1 (proton gradient regulation 1), in a calcium-dependent manner (Terashima *et al.*, 2012; Hertle *et al.*, 2013). There is evidence that FNR is also involved in this pathway, either through direct reduction of the PQ pool using electron flow through Fd, or by acting as a docking site for Fd on the thylakoid membrane (Zhang *et al.*, 2001; Bojko *et al.*, 2003). In green plants, different Fd isoforms have been associated with electron partitioning through LEF/CEF. For instance, specific Fd isoforms that are preferentially involved in CEF have been identified in Arabidopsis (Hanke *et al.*, 2004a; Hanke & Hase, 2008; Voss *et al.*, 2008; Lehtimäki *et al.*, 2010) and maize (Kimata-Ariga *et al.*, 2000). It was suggested that this functional differentiation of Fd isoforms in plants is a result of a nonrecent gene duplication event followed by a selective pressure for binding to components of the CEF pathway, such as PRGL1 or FNR (Goss & Hanke, 2014). The precise nature of CEF in green algae remains elusive, but mutational and crystallography studies have suggested that PETF is the main electron donor to FNR and is thus potentially involved in CEF (Boehm *et al.*, 2016).

Fd-1A and Fd-1B from UWO241 appear to be close homologs to PETF, showing high degrees of similarity in primary sequence (Fig. 2) and tertiary structure (Fig. 3). Furthermore, both proteins contain highly conserved residues important for protein function, including all five residues that form intermolecular salt bridges between Fd and FNR (Kurisu *et al.*, 2001). This indicates that both Fd-1 isoforms from UWO241 have a similar function as described for PETF from *C. reinhardtii*. We identified eight Fd genes in the UWO241 genome, but our data suggest that only the Fd-1 gene is duplicated. We detected Fd genes homologous to all major Fd classes in *C. reinhardtii* (Fig. 6), with the notable exception of Fd-2 and Fd-5. In *C. reinhardtii*, Fd-2 was shown to be involved in state transitions, while Fd-5 plays a role in maintaining thylakoid composition and functionality during growth in the dark ((Winkler *et al.*, 2010; Yang *et al.*, 2015). It appears that the composition of the Fd gene family in UWO241 is different from related mesophilic algae, owing to the extremophilic lifestyle of the psychrophile. We suggest that duplication of the key Fd-1 isoform leads to higher amounts of protein, which could be an adaptive advantage for survival of this alga in its natural environment and might be linked to higher rates of CEF.

Unfortunately, our experimental methods were not able to distinguish between the contributions of Fd-1A vs Fd-1B to cold adaptation in UWO241, as a result of high sequence similarity between the isoforms. To determine if the duplicated Fd genes are under selective pressure, we calculated the ratio of nonsynonymous to synonymous substitutions ($d_N : d_S$) in the Fd proteins. Our data show that both Fd proteins from UWO241 are under purifying selection, suggesting that both gene copies have identical or very similar functions. However, we should stress that when comparing closely related genes with low sequence divergence, such as Fd-1A and Fd-1B, it is difficult to measure a statistically significant divergence from neutral selection based on just a few substitutions. Thus, we cannot exclude the possibility that these different isoforms fulfill separate roles in the psychrophile. For instance, UWO241 is a polyextremophile and has evolved for life under various harsh conditions in addition to low temperature, including extreme shading, high salinity, and high oxygen concentrations. The two Fd-1 isoforms could play different roles under such conditions. Careful experiments characterizing the expression patterns of the two Fd-1 genes under different conditions could provide clues to their specific functions. Furthermore, we cannot eliminate the possibility that both Fd proteins are not equally adapted to function in the cold, and that the activity and stability profiles we observed using purified Fd from UWO241 are a result of different activities and stabilities of the Fd-1 isoforms present in the extract. Functional analysis of recombinantly expressed Fd-1A and Fd-1B would be instrumental in understanding the cold-adapted features of these proteins. Finally, CRISPR-Cas9 editing of the UWO241 genome is under way to generate mutants of UWO241 expressing either Fd-1A or Fd-1B, which would allow us to elucidate the role(s) of photosynthetic Fd in UWO241.

Acknowledgements

N.P.A.H. and D.R.S. are funded by Discovery Grants from the NSERC. N.P.A.H. is grateful for support through the Canadian Foundation for Innovation and The Canada Research Chairs Program.

Author contributions

M.C. and N.P.A.H. conceived and planned the experiments. B.S-M. purified ferredoxin and preformed SDS-PAGE and IEF. M.C. preformed all other experiments and wrote the initial draft of the manuscript. M.P. obtained and assembled the UWO241 transcriptome. P.P. and G.L. performed the protein sequence analyses. D.R.S. devised the genomic and evolutionary analysis. All authors contributed to writing and revising the manuscript.

ORCID

David R. Smith http://orcid.org/0000-0001-9560-5210

References

Aghajari N, Feller G, Gerday C, Haser R. 1998. Structures of the psychrophilic *Alteromonas haloplanctis* α-amylase give insights into cold adaptation at a molecular level. *Structure* **6**: 1503–1516.

Akashi T, Matsumura T, Ideguchi T, Iwakiri K, Kawakatsu T, Taniguchi I, Hase T. 1999. Comparison of the electrostatic binding sites on the surface of ferredoxin for two ferredoxin-dependent enzymes, ferredoxin-NADP$^+$

reductase and sulfite reductase. *Journal of Biological Chemistry* **274**: 29399–29405.

Alvarez M, Zeelen JP, Mainfroid V, Rentier-Delrue F, Martial JA, Wyns L, Wierenga RK, Maes D. 1998. Triose-phosphate isomerase (TIM) of the psychrophilic bacterium *Vibrio marinus:* kinetic and structural properties. *Journal of Biological Chemistry* **273**: 2199–2206.

Åqvist J, Isaksen GV, Brandsdal BO. 2017. Computation of enzyme cold adaptation. *Nature Reviews Chemistry* **1**: 0051.

Atkinson JT, Campbell I, Bennett GN, Silberg JJ. 2016. Cellular assays for ferredoxins: a strategy for understanding electron flow through protein carriers that link metabolic pathways. *Biochemistry* **55**: 7047–7064.

Bertini I, Luchinat C, Provenzani A, Rosato A, Vasos PR. 2002. Browsing gene banks for Fe2S2 ferredoxins and structural modeling of 88 plant-type sequences: an analysis of fold and function. *Proteins* **46**: 110–127.

Boehm M, Alahuhta M, Mulder DW, Peden EA, Long H, Brunecky R, Lunin VV, King PW, Ghirardi ML, Dubini A. 2016. Crystal structure and biochemical characterization of *Chlamydomonas* FDX2 reveal two residues that, when mutated, partially confer FDX2 the redox potential and catalytic properties of FDX1. *Photosynthesis Research* **128**: 45–57.

Bojko M, Kruk J, Więckowski S. 2003. Plastoquinones are effectively reduced by ferredoxin:$NADP^+$ oxidoreductase in the presence of sodium cholate micelles: significance for cyclic electron transport and chlororespiration. *Phytochemistry* **64**: 1055–1060.

Bolger AM, Lohse M, Usadel B. 2014. Trimmomatic: a flexible trimmer for Illumina sequence data. *Bioinformatics* **30**: 2114–2120.

Brown CJ, Todd KM, Rosenzweig RF. 1998. Multiple duplications of yeast hexose transport genes in response to selection in a glucose-limited environment. *Molecular Biology and Evolution* **15**: 931–942.

Chang CH, King PW, Ghirardi ML, Kim K. 2007. Atomic resolution modeling of the ferredoxin:[FeFe] hydrogenase complex from *Chlamydomonas reinhardtii. Biophysical Journal* **93**: 3034–3045.

Chen L, DeVries AL, Cheng C-HC. 1997. Evolution of antifreeze glycoprotein gene from a trypsinogen gene in Antarctic notothenioid fish. *Proceedings of the National Academy of Sciences, USA* **94**: 3811–3816.

Chen Z, Cheng C-HC, Zhang J, Cao L, Chen L, Zhou L, Jin Y, Ye H, Deng C, Dai Z *et al.* 2008. Transcriptomic and genomic evolution under constant cold in Antarctic notothenioid fish. *Proceedings of the National Academy of Sciences, USA* **105**: 12944–12949.

Christ D, Chin JW. 2008. Engineering *Escherichia coli* heat-resistance by synthetic gene amplification. *Protein Engineering, Design and Selection* **21**: 121–125.

Collins T, Roulling F, Piette F, Marx J-C, Feller G, Gerday C, D'Amico S. 2008. Fundamentals of cold-adapted enzymes. In: Margesin R, Schinner F, Marx J-C, Gerday C, eds. *Psychrophiles: from biodiversity to biotechnology.* Berlin, Heidelberg, Germany: Springer, 211–227.

Conant GC, Wolfe KH. 2008. Turning a hobby into a job: how duplicated genes find new functions. *Nature Reviews Genetics* **9**: 938–950.

Cvetkovska M, Hüner NPA, Smith DR. 2017. Chilling out: the evolution and diversification of psychrophilic algae with a focus on Chlamydomonadales. *Polar Biology* **40**: 1169–1184.

D'Amico S, Claverie P, Collins T, Georlette D, Gratia E, Hoyoux A, Meuwis M-A, Feller G, Gerday C. 2002. Molecular basis of cold adaptation. *Philosophical Transactions of the Royal Society B: Biological Sciences* **357**: 917–925.

D'Amico S, Marx J-C, Gerday C, Feller G. 2003. Activity-stability relationships in extremophilic enzymes. *Journal of Biological Chemistry* **278**: 7891–7896.

Dassanayake M, Oh D-H, Haas JS, Hernandez A, Hong H, Ali S, Yun D-J, Bressan RA, Zhu J-K, Bohnert HJ *et al.* 2011. The genome of the extremophile crucifer *Thellungiella parvula. Nature genetics* **43**: 913–918.

De Maayer P, Anderson D, Cary C, Cowan DA. 2014. Some like it cold: understanding the survival strategies of psychrophiles. *EMBO reports* **15**: 508–517.

DeBolt S. 2010. Copy number variation shapes genome diversity in *Arabidopsis* over immediate family generational scales. *Genome Biology and Evolution* **2**: 441–453.

Devos N, Ingouff M, Loppes R, Matagne RF. 1998. RuBisCo adaptation to low temperatures: a comparative study in psychrophilic and mesophilic unicellular algae. *Journal of Phycology* **34**: 655–660.

Di Martino Rigano V, Vona V, Lobosco O, Carillo P, Lunn JE, Carfagna S, Esposito S, Caiazzo M, Rigano C. 2006. Temperature dependence of nitrate reductase in the psychrophilic unicellular alga *Koliella antarctica* and the mesophilic alga *Chlorella sorokiniana. Plant, Cell & Environment* **29**: 1400–1409.

Dolhi JM, Maxwell DP, Morgan-Kiss RM. 2013. Review: the Antarctic *Chlamydomonas raudensis*: an emerging model for cold adaptation of photosynthesis. *Extremophiles* **17**: 711–722.

Edgar RC. 2004. MUSCLE: multiple sequence alignment with high accuracy and high throughput. *Nucleic Acids Research* **32**: 1792–1797.

Ewen KM, Ringle M, Bernhardt R. 2012. Adrenodoxin – a versatile ferredoxin. *IUBMB Life* **64**: 506–512.

Feller G. 2013. Psychrophilic enzymes: from folding to function and biotechnology. *Scientifica* **2013**: 1–28.

Feller G, Gerday C. 2003. Psychrophilic enzymes: hot topics in cold adaptation. *Nature Reviews Microbiology* **1**: 200–208.

Ferrara M, Guerriero G, Cardi M, Esposito S. 2013. Purification and biochemical characterisation of a glucose-6-phosphate dehydrogenase from the psychrophilic green alga *Koliella antarctica. Extremophiles* **17**: 53–62.

Fukuyama K. 2004. Structure and function of plant-type ferredoxins. *Photosynthesis research* **81**: 289–301.

García-Sánchez MI, Díaz-Quintana A, Gotor C, Jacquot J-P, De la Rosa MA, Vega JM. 2000. Homology predicted structure and functional interaction of ferredoxin from the eukaryotic alga *Chlamydomonas reinhardtii* with nitrite reductase and glutamate synthase. *JBIC Journal of Biological Inorganic Chemistry* **5**: 713–719.

Goss T, Hanke G. 2014. The end of the line: can ferredoxin and ferredoxin NADP(H) oxidoreductase determine the fate of photosynthetic electrons? *Current Protein and Peptide Science* **15**: 385–393.

Grabherr MG, Haas BJ, Yassour M, Levin JZ, Thompson DA, Amit I, Adiconis X, Fan L, Raychowdhury R, Zeng Q *et al.* 2011. Full-length transcriptome assembly from RNA-Seq data without a reference genome. *Nature Biotechnology* **29**: 644–652.

Greenfield NJ. 2006. Using circular dichroism collected as a function of temperature to determine the thermodynamics of protein unfolding and binding interactions. *Nature protocols* **1**: 2527–2535.

Hahn MW. 2009. Distinguishing among evolutionary models for the maintenance of gene duplicates. *Journal of Heredity* **100**: 605–617.

Hanke G, Mulo P. 2013. Plant type ferredoxins and ferredoxin-dependent metabolism: chloroplast ferredoxins. *Plant, Cell & Environment* **36**: 1071–1084.

Hanke GT, Hase T. 2008. Variable photosynthetic roles of two leaf-type ferredoxins in *Arabidopsis*, as revealed by RNA interference. *Photochemistry and Photobiology* **84**: 1302–1309.

Hanke GT, Kimata-Ariga Y, Taniguchi I, Hase T. 2004a. A post genomic characterization of *Arabidopsis* ferredoxins. *Plant Physiology* **134**: 255–264.

Hanke GT, Kurisu G, Kusunoki M, Hase T. 2004b. Fd: FNR electron transfer complexes: evolutionary refinement of structural interactions. *Photosynthesis research* **81**: 317–327.

Hertle AP, Blunder T, Wunder T, Pesaresi P, Pribil M, Armbruster U, Leister D. 2013. PGRL1 is the elusive ferredoxin-plastoquinone reductase in photosynthetic cyclic lectron flow. *Molecular Cell* **49**: 511–523.

Innan H, Kondrashov F. 2010. The evolution of gene duplications: classifying and distinguishing between models. *Nature Reviews Genetics* **11**: 97–108.

Iwai M, Takizawa K, Tokutsu R, Okamuro A, Takahashi Y, Minagawa J. 2010. Isolation of the elusive supercomplex that drives cyclic electron flow in photosynthesis. *Nature* **464**: 1210–1213.

James TC, Usher J, Campbell S, Bond U. 2008. Lager yeasts possess dynamic genomes that undergo rearrangements and gene amplification in response to stress. *Current Genetics* **53**: 139–152.

Kameda H, Hirabayashi K, Wada K, Fukuyama K. 2011. Mapping of protein-protein interaction sites in the plant-type [2Fe-2S] ferredoxin. *PLoS ONE* **6**: e21947.

Kelley DR, Schatz MC, Salzberg SL. 2010. Quake: quality-aware detection and correction of sequencing errors. *Genome Biology* **11**: R116.

Kelley LA, Mezulis S, Yates CM, Wass MN, Sternberg MJE. 2015. The Phyre2 web portal for protein modeling, prediction and analysis. *Nature Protocols* **10**: 845–858.

Kimata-Ariga Y, Matsumura T, Kada S, Fujimoto H, Fujita Y, Endo T, Mano J, Sato F, Hase T. 2000. Differential electron flow around photosystem I by two C_4-photosynthetic-cell-specific ferredoxins. *The EMBO Journal* **19**: 5041–5050.

Kondrashov FA. 2012. Gene duplication as a mechanism of genomic adaptation to a changing environment. *Proceedings of the Royal Society B: Biological Sciences* **279**: 5048–5057.

Kurisu G, Kusunoki M, Katoh E, Yamazaki T, Teshima K, Onda Y, Kimata-Ariga Y, Hase T. 2001. Structure of the electron transfer complex between ferredoxin and ferredoxin-NADP$^+$ reductase. *Nature Structural & Molecular Biology* **8**: 117–121.

Kuwajima K. 1989. The molten globule state as a clue for understanding the folding and cooperativity of globular-protein structure. *Proteins: Structure Function, and Bioinformatics* **6**: 87–103.

Lehtimäki N, Lintala M, Allahverdiyeva Y, Aro E-M, Mulo P. 2010. Drought stress-induced upregulation of components involved in ferredoxin-dependent cyclic electron transfer. *Journal of Plant Physiology* **167**: 1018–1022.

Loppes R, Devos N, Willem S, Barthélemy P, Matagne RF. 1996. Effect of temperature on two enzymes from a psychrophilic *Chloromonas* (chlorophyta). *Journal of Phycology* **32**: 276–278.

Lynch M, Conery JS. 2000. The evolutionary fate and consequences of duplicate genes. *Science* **290**: 1151–1155.

Maeda M, Lee YH, Ikegami T, Tamura K, Hoshino M, Yamazaki T, Nakayama M, Hase T, Goto Y. 2005. Identification of the N- and C-terminal substrate binding segments of ferredoxin-NADP$^+$ reductase by NMR. *Biochemistry* **44**: 10644–10653.

Martin M. 2011. Cutadapt removes adapter sequences from high-throughput sequencing reads. *EMBnet Journal* **17**: 10–12.

Menke M, Berger B, Cowen L. 2008. Matt: local flexibility aids protein multiple structure alignment. *PLoS Computational Biology* **4**: e10.

Miyake C. 2010. Alternative electron flows (water-water cycle and cyclic electron flow around PSI) in photosynthesis: Molecular mechanisms and physiological functions. *Plant and Cell Physiology* **51**: 1951–1963.

Morgan RM, Ivanov AG, Priscu JC, Maxwell DP, Huner NP. 1998. Structure and composition of the photochemical apparatus of the Antarctic green alga, *Chlamydomonas subcaudata*. *Photosynthesis Research* **56**: 303–314.

Morgan-Kiss RM, Ivanov AG, Huner NP. 2002. The Antarctic psychrophile, *Chlamydomonas subcaudata*, is deficient in state I–state II transitions. *Planta* **214**: 435–445.

Morgan-Kiss RM, Priscu JC, Pocock T, Gudynaite-Savitch L, Huner NPA. 2006. Adaptation and acclimation of photosynthetic microorganisms to permanently cold environments. *Microbiology and Molecular Biology Reviews* **70**: 222–252.

Müller JJ, Müller A, Rottmann M, Bernhardt R, Heinemann U. 1999. Vertebrate-type and plant-type ferredoxins: crystal structure comparison and electron transfer pathway modelling. *Journal of molecular biology* **294**: 501–513.

Narinx E, Baise E, Gerday C. 1997. Subtilisin from psychrophilic antarctic bacteria: characterization and site-directed mutagenesis of residues possibly involved in the adaptation to cold. *Protein Engineering* **10**: 1271–1279.

Neale PJ, Priscu JC. 1995. The Photosynthetic apparatus of phytoplankton from a perennially ice-covered Antarctic lake: acclimation to an extreme shade environment. *Plant and Cell Physiology* **36**: 253–263.

Noguchi A, Nishino T, Nakayama T. 2009. Kinetic and thermodynamic characterization of the cold activity acquired upon single amino-acid substitution near the active site of a thermostable α-glucosidase. *Journal of Molecular Catalysis B: Enzymatic* **56**: 300–306.

Oh D-H, Dassanayake M, Bohnert HJ, Cheeseman JM. 2012. Life at the extreme: lessons from the genome. *Genome biology* **13**: 241.

Peden EA, Boehm M, Mulder DW, Davis R, Old WM, King PW, Ghirardi ML, Dubini A. 2013. Identification of global ferredoxin interaction networks in *Chlamydomonas reinhardtii*. *Journal of Biological Chemistry* **288**: 35192–35209.

Pettersen EF, Goddard TD, Huang CC, Couch GS, Greenblatt DM, Meng EC, Ferrin TE. 2004. UCSF Chimera – a visualization system for exploratory research and analysis. *Journal of Computational Chemistry* **25**: 1605–1612.

Pocock TH, Koziak A, Rosso D, Falk S, Hüner NPA. 2007. *Chlamydomonas raudensis* (UWO 241), Chlorophyceae, exhibits the capacity for rapid D1 repair in response to chronic photoinhibition at low temperature. *Journal of Phycology* **43**: 924–936.

Pocock T, Lachance M-A, Pröschold T, Priscu JC, Kim SS, Huner NPA. 2004. Identification of a psychrophilic green alga from Lake Bonney, Antarctica: *Chlamydomonas raudensis* Ettl. (UWO 241) Chlorophyceae. *Journal of Phycology* **40**: 1138–1148.

Possmayer M, Berardi G, Beall BFN, Trick CG, Hüner NPA, Maxwell DP. 2011. Plasticity of the psychrophilic green algae *Chlamydomonas raudensis* (UWO 241) (Chlorophyta) to supraoptimal temperature stress. *Journal of Phycology* **47**: 1098–1109.

Possmayer M, Gupta RK, Szyszka-Mroz B, Maxwell DP, Lachance M, Hüner NPA, Smith DR. 2016. Resolving the phylogenetic relationship between *Chlamydomonas* sp. UWO 241 and *Chlamydomonas raudensis* sag 49.72 (Chlorophyceae) with nuclear and plastid DNA sequences. *Journal of Phycology* **52**: 305–310.

Rochaix J-D. 2014. Regulation and dynamics of the light-harvesting system. *Annual Review of Plant Biology* **65**: 287–309.

von Rozycki T, Nies DH. 2009. *Cupriavidus metallidurans*: evolution of a metal-resistant bacterium. *Antonie van Leeuwenhoek* **96**: 115.

Rumpel S, Siebel JF, Diallo M, Farès C, Reijerse EJ, Lubitz W. 2015. Structural insight into the complex of ferredoxin and [FeFe] hydrogenase from *Chlamydomonas reinhardtii*. *ChemBioChem* **16**: 1663–1669.

Saitoh T, Ikegami T, Nakayama M, Teshima K, Akutsu H, Hase T. 2006. NMR Study of the electron transfer complex of plant ferredoxin and sulfite reductase: mapping the interaction sites of ferredoxin. *Journal of Biological Chemistry* **281**: 10482–10488.

Sakakibara Y, Kimura H, Iwamura A, Saitoh T, Ikegami T, Kurisu G, Hase T. 2012. A new structural insight into differential interaction of cyanobacterial and plant ferredoxins with nitrite reductase as revealed by NMR and X-ray crystallographic studies. *Journal of Biochemistry* **151**: 483–492.

Sawyer A, Winkler M. 2017. Evolution of *Chlamydomonas reinhardtii* ferredoxins and their interactions with [FeFe]-hydrogenases. *Photosynthesis Research* **134**: 307–316.

Schmitter J-M, Jacquot J-P, de Lamotte-Guery F, Beauvallet C, Dutka S, Gadal P, Decottignies P. 1988. Purification, properties and complete amino acid sequence of the ferredoxin from a green alga, *Chlamydomonas reinhardtii*. *European Journal of Biochemistry* **172**: 405–412.

Shikanai T. 2007. Cyclic electron transport around photosystem I: genetic approaches. *Annual Review of Plant Biology* **58**: 199–217.

Siddiqui KS. 2017. Defying the activity–stability trade-off in enzymes: taking advantage of entropy to enhance activity and thermostability. *Critical Reviews in Biotechnology* **37**: 309–322.

Siddiqui KS, Cavicchioli R. 2006. Cold-adapted enzymes. *Annual Review of Biochemistry* **75**: 403–433.

Siddiqui KS, Williams TJ, Wilkins D, Yau S, Allen MA, Brown MV, Lauro FM, Cavicchioli R. 2013. Psychrophiles. *Annual Review of Earth and Planetary Sciences* **41**: 87–115.

Sievers F, Wilm A, Dineen D, Gibson TJ, Karplus K, Li W, Lopez R, McWilliam H, Remmert M, Söding J *et al.* 2011. Fast, scalable generation of high-quality protein multiple sequence alignments using Clustal Omega. *Molecular Systems Biology* **7**: 539.

Simpson JT, Wong K, Jackman SD, Schein JE, Jones SJM, Birol İ. 2009. ABySS: a parallel assembler for short read sequence data. *Genome Research* **19**: 1117–1123.

Stranger BE, Forrest MS, Dunning M, Ingle CE, Beazley C, Thorne N, Redon R, Bird CP, de Grassi A, Lee C *et al.* 2007. Relative impact of nucleotide and copy number variation on gene expression phenotypes. *Science* **315**: 848–853.

Szyszka B, Ivanov AG, Hüner NPA. 2007. Psychrophily is associated with differential energy partitioning, photosystem stoichiometry and polypeptide

phosphorylation in *Chlamydomonas raudensis*. *Biochimica et Biophysica Acta (BBA) – Bioenergetics* **1767**: 789–800.

Szyszka-Mroz B, Pittock P, Ivanov AG, Lajoie G, Hüner NPA. 2015. The Antarctic Psychrophile *Chlamydomonas* sp. UWO 241 preferentially phosphorylates a photosystem I-cytochrome b_6f supercomplex. *Plant Physiology* **169**: 717–736.

Takizawa K, Takahashi S, Hüner NPA, Minagawa J. 2009. Salinity affects the photoacclimation of *Chlamydomonas raudensis* Ettl UWO241. *Photosynthesis Research* **99**: 195–203.

Terashima M, Petroutsos D, Hüdig M, Tolstygina I, Trompelt K, Gäbelein P, Fufezan C, Kudla J, Weinl S, Finazzi G *et al.* 2012. Calcium-dependent regulation of cyclic photosynthetic electron transfer by a CAS, ANR1, and PGRL1 complex. *Proceedings of the National Academy of Sciences, USA* **109**: 17717–17722.

Terauchi AM, Lu S-F, Zaffagnini M, Tappa S, Hirasawa M, Tripathy JN, Knaff DB, Farmer PJ, Lemaire SD, Hase T *et al.* 2009. Pattern of expression and substrate specificity of chloroplast ferredoxins from *Chlamydomonas reinhardtii*. *Journal of Biological Chemistry* **284**: 25867–25878.

Vona V, Di Martino Rigano V, Lobosco O, Carfagna S, Esposito S, Rigano C. 2004. Temperature responses of growth, photosynthesis, respiration and NADH: nitrate reductase in cryophilic and mesophilic algae. *New Phytologist* **163**: 325–331.

Voss I, Koelmann M, Wojtera J, Holtgrefe S, Kitzmann C, Backhausen JE, Scheibe R. 2008. Knockout of major leaf ferredoxin reveals new redox-regulatory adaptations in *Arabidopsis thaliana*. *Physiologia Plantarum* **133**: 584–598.

Winkler M, Hemschemeier A, Jacobs J, Stripp S, Happe T. 2010. Multiple ferredoxin isoforms in *Chlamydomonas reinhardtii* – their role under stress conditions and biotechnological implications. *European Journal of Cell Biology* **89**: 998–1004.

Winkler M, Kuhlgert S, Hippler M, Happe T. 2009. Characterization of the key step for light-driven hydrogen evolution in green algae. *Journal of Biological Chemistry* **284**: 36620–36627.

Yang Z. 2007. PAML 4: phylogenetic analysis by maximum likelihood. *Molecular Biology and Evolution* **24**: 1586–1591.

Yang Z, Bielawski JP. 2000. Statistical methods for detecting molecular adaptation. *Trends in Ecology & Evolution* **15**: 496–503.

Yang F, Pecina DA, Kelly SD, Kim S-H, Kemner KM, Long DT, Marsh TL. 2010. Biosequestration via cooperative binding of copper by *Ralstonia pickettii*. *Environmental Technology* **31**: 1045–1060.

Yang W, Wittkopp TM, Li X, Warakanont J, Dubini A, Catalanotti C, Kim RG, Nowack ECM, Mackinder LCM, Aksoy M *et al.* 2015. Critical role of *Chlamydomonas reinhardtii* ferredoxin-5 in maintaining membrane structure and dark metabolism. *Proceedings of the National Academy of Sciences, USA* **112**: 14978–14983.

Zhang H, Whitelegge JP, Cramer WA. 2001. Ferredoxin:NADP$^+$ oxidoreductase is a subunit of the chloroplast cytochrome b6f complex. *Journal of Biological Chemistry* **276**: 38159–38165.

Zhou D, Zhou J, Meng L, Wang Q, Xie H, Guan Y, Ma Z, Zhong Y, Chen F, Liu J. 2009. Duplication and adaptive evolution of the COR15 genes within the highly cold-tolerant *Draba* lineage (Brassicaceae). *Gene* **441**: 36–44.

Zhou J, Lemos B, Dopman EB, Hartl DL. 2011. Copy-number variation: the balance between gene dosage and expression in *Drosophila melanogaster*. *Genome Biology and Evolution* **3**: 1014–1024.

Supporting Information

Additional Supporting Information may be found online in the Supporting Information tab for this article:

Fig. S1 Enzyme kinetics for the activity of photosynthetic ferredoxin from *Spinacia oleracea*, *Chlamydomonas reinhardtii* and *Chlamydomonas* sp. UWO241 during the reduction of cytochrome c using ferredoxin NADPH reductase (FNR) from *S. oleracea*.

Fig. S2 Immunoblot of increasing concentration of total proteins from *Chlamydomonas reinhardtii* and *Chlamdyomonas* sp. UWO241, probed with antibody specific for ferredoxin.

Fig. S3 A model showing the predicted tertiary structures of the two ferredoxin isoforms from *Chlamydomonas* sp. UWO241 (Fd-1A, Fd-1B), superimposed to the structure of other green algae, plants and cyanobacteria.

Fig. S4 Multiple alignment of predicted ferredoxin amino acid sequences from *Chlamydomonas* sp. UWO241, obtained by screening the genome using BLAST searches with known Fd sequences from *Chlamydomonas reinhardtii*, and other related algae and plant species.

Fig. S5 The change in secondary structure of purified photosynthetic ferredoxin from *Chlamydomonas reinhardtii* and *Chlamydomonas* sp. UWO241 exposure to 10, 40, and 60°C.

Fig. S6 The gene structure of ferredoxin genes from *Chlamydomonas* sp. UWO241 and closely related green algae.

Table S1 PEAKS results for purified ferredoxin of *Chlamydomonas* sp. UWO24

Please note: Wiley Blackwell are not responsible for the content or functionality of any Supporting Information supplied by the authors. Any queries (other than missing material) should be directed to the *New Phytologist* Central Office.